PB-237 745

NO2 ACTINOMETER FOR FIELD USE

Darrell E. Burch, et al

Philco-Ford Corporation

Prepared for:

National Environmental Research Center

August 1974

DISTRIBUTED BY:

NTIS

National Technical Information Service
U. S. DEPARTMENT OF COMMERCE

TECHNICAL REPORT DATA
(Please read Instructions on the reverse before com

PB 237 745

1. REPORT NO. EPA-650/4-74-036	2.
4. TITLE AND SUBTITLE NO_2 Actinometer for Field Use	5. REPORT DATE August 1974
	6. PERFORMING ORGANIZATION CODE
7. AUTHOR(S) Darrell E. Burch, Ross C. Bean and Francis J. Gates	8. PERFORMING ORGANIZATION REPORT NO. U-6074
9. PERFORMING ORGANIZATION NAME AND ADDRESS Philco-Ford, Aeronutronic Division, Ford Road Newport Beach, California 92663	10. PROGRAM ELEMENT NO. 1A1003
	11. CONTRACT/GRANT NO. 68-02-0798
12. SPONSORING AGENCY NAME AND ADDRESS National Environmental Research Center Research Triangle Park, N. C. 27711	13. TYPE OF REPORT AND PERIOD COVERED
	14. SPONSORING AGENCY CODE

15. SUPPLEMENTARY NOTES

16. ABSTRACT

Solar radiant energy in the ultraviolet and short-wavelength visible dissociate NO_2 in the atmosphere to produce NO and O_2. This photolytic reaction plays an important role in the formation of photochemical smog, and information about the amount of actinic energy available in the lower atmosphere is required for the development of mathematical models of the atmospheric processes. This report describes the development and testing of an actinometer designed to measure the actinic energy available for the photolytic dissociation of NO_2. A spherical test bulb contains a mixture of NO_2 and O_2 when it has been in the dark for several minutes. When the bulb is exposed to solar energy NO is formed; its concentration is monitored by gas-cell correlation methods involving the infrared absorption by NO. A shutter periodically shades the test bulb from the sun for a one-minute period each two minutes. During the shaded period, part of the NO recombines with O_2 to form NO_2. The cyclic change in the NO concentration is related to the actinic irradiance.

17. KEY WORDS AND DOCUMENT ANALYSIS

a. DESCRIPTORS	b. IDENTIFIERS/OPEN-ENDED TERMS	c. COSATI Field/Group
Actinometer Nitric Oxide Nitrogen Dioxide		

18. DISTRIBUTION STATEMENT Unlimited	19. SECURITY CLASS (This Report) Unclassified	21. NO. OF PAGES 55
	20. SECURITY CLASS (This page) Unclassified	22. PRICE $4.25/2.25

EPA Form 2220-1 (9-73)

Reproduced by
NATIONAL TECHNICAL
INFORMATION SERVICE
U S Department of Commerce
Springfield VA 22151

EPA-650/4-74-036

NO_2 ACTINOMETER FOR FIELD USE

Prepared by

D.E. Burch, R.C. Bean, and F.J. Gates

Philco-Ford Co., Aeronutronic Division,
Ford Road
Newport Beach, California 92663

Contract No. 68-02-0798
ROAP No. 56AAI
Program Element No. 1A1003

EPA Project Officer: P.L. Hanst

Chemistry and Physics Laboratory
National Environmental Research Center
Research Triangle Park, North Carolina 27711

Prepared for

OFFICE OF RESEARCH AND DEVELOPMENT
U.S. ENVIRONMENTAL PROTECTION AGENCY
WASHINGTON, D.C. 20460

August 1974

1a

This report has been reviewed by the Environmental Protection Agency and approved for publication. Approval does not signify that the contents necessarily reflect the views and policies of the Agency, nor does mention of trade names or commercial products constitute endorsement or recommendation for use.

ABSTRACT

Solar radiant energy in the ultraviolet and short-wavelength visible dissociate NO_2 in the atmosphere to produce NO and O_2. This photolytic reaction plays an important role in the formation of photochemical smog, and information about the amount of actinic energy available in the lower atmosphere is required for the development of mathematical models of the atmospheric processes. This report describes the development and testing of an actinometer designed to measure the actinic energy available for the photolytic dissociation of NO2. A spherical test bulb contains a mixture of NO_2 and O_2 when it has been in the dark for several minutes. When the bulb is exposed to solar energy NO is formed; its concentration is monitored by gas-cell correlation methods involving the infrared absorption by NO. A shutter periodically shades the test bulb from the sun for a one-minute period each two minutes. During the shaded period, part of the NO recombines with O_2 to form NO_2. The cyclic change in the NO concentration is related to the actinic irradiance.

FIGURES

No.		Page
1-1	Spectral plots of the absorption coefficient$_o$ for NO_2 and N_2O_4 between 3000 cm^{-1} and 4500 A	1-5
2-1	Optical diagram of actinometer used for preliminary tests	2-2
2-2	Response of breadboard model NO_2 actinometer to sunlight	2-5
2-3	Response of NO_2 actinometer to artificial uv and visible light at different intensities and different position in the test bulb	2-6
2-4	Plots of V" and ΔV" vs relative actinic irradiance	2-8
2-5	Plots of V" and ΔV" vs O_2 partial pressure in the test bulb for various partial pressures of NO_2	
2-6	Transmittance of NO_2 from 4300 to 4500 $\mathring{A}$	2-12
3-1	Optical diagrams of the optics assembly of the actinometer	3-2
3-2	Two views of the optics assembly of the actinometer	3-3
3-3	Photograph of the control assembly, amplifier and recorder	3-4
4-1	Response of actinometer to solar energy with the shutter in the automatic mode	4-2
4-2	Recorder tracings of actinometer output when the sky contains broken clouds	4-3

FIGURES (contd.)

No.		Page
4-3	Plots of $\Delta V''$ vs relative actinic irradiance	4-5
4-4	Response of actinometer to different absorber thicknesses of NO in a mixture of NO + N_2 at a total pressure of 120 torr	4-8
5-1	Simplified schematic diagram for ac power	5-4
5-2	Simplified diagram of interconnecting cables	5-5
5-3	Wiring diagram of electrical components on the optics assembly	5-5
5-4	Wiring diagram of timer and control assembly	5-6
5-5	Schematic diagram of preamplifier used with the InSb detector	5-7
5-6	Schematic diagram of the 350 Hz reference-pickup	5-7
5-7	Power supply for thermo-electric cooler for the detector	5-8
5-8	Power supply for preamp and reference circuits	5-8

SECTION 1

INTRODUCTION

BACKGROUND

Nitrogen dioxide is readily photolyzed to NO and O_2 by short-wave visible and near-ultraviolet light. Measurement of the rate of photolysis of NO_2 in polluted air is necessary in order to understand the complex photochemical processes in the atmosphere. Photolysis of NO_2 starts a series of chemical reactions that yield ozone, peroxyacyl nitrates, and other objectionable species that make up photochemical smog. There is presently a need for a field instrument that can measure the amount of light available to photolyze NO_2 for purposes of developing mathematical models of the atmospheric processes.

Laboratory methods for measuring the intensity of light producing photolysis usually involve a photochemical reaction chamber containing NO_2 and an inert gas. The photolysis is measured by monitoring the disappearance of NO_2. Such a method is impractical for a field instrument because the gas must be replaced after each measurement. Photoelectric instruments have generally been used in the field because they are simple and can be used continuously. However, this type of instrument suffers two serious drawbacks that make it difficult to relate a reading to the rate of NO_2 photolysis.

Geometric corrections and spectral response corrections must be applied to the reading of the photoelectric sensor. The response of a photodetector is highly directional, with maximum response to light rays perpendicular to the surface. It is clear that correcting for the directional response would be quite complicated and would require considerable knowledge of the angular variation of the solar irradiance, which depends on the solar zenith angle and on the conditions of clouds and haze.

Spectral corrections are required because it is not possible to produce a photodetector surface with a spectral response that matches the absorption spectrum of NO_2. The rate of photolysis due to light in a narrow spectral interval is proportional to the product of the solar spectral irradiance and the absorptivity of the NO_2. Similarly, the response of a photodetector due to the same narrow spectral interval is proportional to the product of the solar irradiance and the spectral responsivity of the detector. Because the relative spectral responsivity of a photodetector may change and the spectrum of sunlight reaching the lower atmosphere is variable, the spectral correction is also very difficult.

SUGGESTED INSTRUMENT FEATURES

An ideal NO_2 actinometer would have exactly the same spectral response as the NO_2 absorption in the atmosphere and would be equally sensitive to light arriving from any direction. Hanst[1] has suggested that this ideal actinometer can be approximated by an instrument built along the following lines. A spherical receiver, which we shall call a test bulb, is made of quartz, which is transparent to all wavelengths of actinic radiant energy reaching the lower atmosphere. A photosensitive mixture of $NO_2 + O_2$, and possibly an inert gas such as N_2, is contained in the test bulb. The system operation depends on the chemistry of NO_2 photolysis and the reverse reaction given by

$$NO_2 + h\nu \rightleftharpoons NO + (1/2)\ O_2. \qquad (1\text{-}1)$$

The bulb is mounted in the open, well above any parts of the instrument, so it can receive radiant energy from all directions except for a few steradians below. Most types of earth surface reflect weakly in the uv and visible; therefore, it is unlikely that a significant fraction of the actinic energy reaching a point in the lower atmosphere comes from the lower hemisphere. Thus, the gas in the bulb will effectively integrate the effects of the radiant energy arriving from all directions.

The problem of spectral response errors inherent in photoelectric detectors is greatly reduced by having the NO_2 itself be the absorber of actinic light in the actinometer. Since the absorptivity of NO_2 is not the same for all wavelengths of actinic light, the correct spectral response can be maintained only if the NO_2 concentration in the test bulb is low enough that the gas is optically thin at all wavelengths.

A new feature of the instrument suggested by Hanst involves the addition of O_2 to the test bulb along with the NO_2. In the presence of the excess O_2 the reverse reaction takes place to form NO_2 when the test bulb

is shaded from actinic light. The second new feature of the suggested instrument is a shutter that periodically opens to expose the test bulb to actinic light then closes to allow the reverse reaction to occur. The increase in the concentration of the NO, or the decrease in NO_2, during the open portion of each cycle of the shutter is monitored spectroscopically. The monitor employs a gas correlation cell that is used as a selective filter. The correlation cell contains either NO or NO_2, whichever is being monitored in the test bulb.

We have previously employed gas correlation methods to monitor NO at concentrations of interest for the present purposes. The fundamental vibration-rotation absorption band near 5.4 μm is employed. The fractional change in the NO concentration in the test bulb is expected to be quite large during each period of the cyclic shutter. On the other hand, only a small fraction of the NO_2 is expected to dissociate during each cycle. Therefore, it seemed likely that the NO concentration could be measured more accurately than the NO_2 concentration. Monitoring NO_2 has one advantage in that visible absorption bands could be employed to take advantage of simple and efficient sources and detectors.

SUMMARY OF WORK PERFORMED

The objectives of the work reported here have been to demonstrate the feasibility of an NO_2 actinometer based on Hanst's recommendations, to perform experiments to determine the required design parameters, and to build and demonstrate an instrument for field use and evaluation. The preliminary tests performed before the final instrument was designed are discussed in Section 2. Most of the tests were performed indoors under controlled conditions with a uv lamp serving as the source of actinic energy. Gas cell correlation methods were used to monitor the NO concentration in a cylindrical test bulb. A cylindrical bulb, rather than a spherical one, was used because it facilitated the investigation of possible wall effects and geometrical effects in the test bulb. Besides demonstrating the feasibility of the instrument, the preliminary tests provided information that was quite valuable in the design of the actinometer to be built and demonstrated as part of the present contract.

Limited experimental data obtained on the measurement of NO_2 by gas correlation methods tended to confirm our original belief that NO could be better monitored in an actinometer test bulb than could NO_2. A few data were obtained by using hot NO as a source of radiant energy when monitoring NO in a separate sample. As expected, a given small sample of NO produces a larger fractional change in the detector signal when hot NO is used as an energy source in the place of a continuum source. Better discrimination against interfering H_2O absorption can also be achieved. However, simple NO cells cannot be operated at temperatures as high as conventional continuum sources; therefore, their spectral radiance is less,

even at wavelengths of high NO emissivity. We have chosen a hot ceramic source for the actinometer because of its simplicity and the improved signal-to-noise ratio obtainable with it.

Section 3 describes the actinometer built for laboratory and field use. It has been designed so that components can be interchanged and gas mixtures in the correlation cell and test bulb can be modified. Only a limited amount of test data represented by those summarized in Section 4 have been obtained. Although the practicality of the instrument for field use has been demonstrated and the tests indicate that it performs adequately, subsequent tests to be performed by EPA scientists will probably lead to suggestions for minor design changes.

SPECTRAL CHARACTERISTICS OF NO_2 ABSORPTION

When actinic radiant energy strikes a layer of NO_2, the absorption is a function of the wavelength with strong absorption throughout much of the visible and near uv. N_2O_4, a compound that is always associated with NO_2, is transparent in the visible but absorbs in the uv. Fig. 1-1 shows plots of the absorption coefficients as given by Leighton[2] for both species over this portion of the spectrum. The spectral curves shown in Fig. 1-1 were not obtained with sufficiently good resolution to show all of the vibrational structure that exists at the longer wavelengths. Below about 3700Å the bands are diffuse with essentially no unresolved structure.

If $I_{o,\lambda}$ photons of actinic energy of wavelength λ in a parallel beam are incident on each cm^2 per second, the rate of absorption of the photons is given by

$$N_a(\text{photons } cm^{-3} sec^{-1}) = \int \alpha C I_{o,\lambda} d\lambda, \qquad (1\text{-}2)$$

where α, the absorption coefficient, is expressed in cm^2/molecule and is a function of wavelength, and C is the concentration of the absorbing gas species in molecules/cm^3. Equation (1-2) is restricted to optically thin samples so that the incident intensity is essentially the same at all points in the absorbing layer. If the sample is too thick, the intensity is less near the surface where the beam leaves the absorbing layer than it is on the front surface where the beam is incident. Additional data on NO_2 absorption in the visible appear in Section 2.

The absorption coefficient shown as the right-hand ordinate scale of Fig. 1-1 is expressed in $atm^{-1}cm^{-1}$ and is convenient when relating the transmittance to the amount of NO_2 in the optical path. If p is the partial pressure of the absorbing gas in atmospheres, θ is the temperature in degrees Kelvin, and L is the geometrical path length through the gas,

$$I_\lambda = \exp - \left[\beta_\lambda \ (\text{atm}^{-1}\text{cm}^{-1}{}_{\text{STP}}) \ p(\text{atm}) \ L(\text{cm}) \ 273/\theta\right]. \qquad (1\text{-}3)$$

The ratio of the concentration of N_2O_4 to that of NO_2 decreases with increasing temperature and increases in proportion to the NO_2 pressure. Because of the very low partial pressure of NO_2 in the atmosphere, the fraction that appears as N_2O_4 is extremely low and, therefore, negligible. However, the N_2O_4 absorption may be significant in laboratory samples or in test cells containing higher concentrations of the gases. The relative equilibrium concentrations of NO_2 and N_2O_4 can be determined from data given by Giauque and Kemp[3].

Most of the absorbed radiant energy of wavelengths greater than approximately 4100Å produces changes in the electronic and vibrational energies of the absorbing molecules, but it does not produce dissociation. However, a large fraction of the energy of shorter wavelengths produces photolysis of the NO_2 molecules in accordance with Eq. (1-1). The quantum yields of photolysis, according to Leighton at 4 representative wavelengths are as follows: 3130Å, 0.97; 3660Å, 0.92; 4047Å, 0.36; and 4358Å, 0.00. Because of the low quantum yield of photolysis at the longer wavelengths and the low spectral radiance of the sun at short wavelengths, most of the photolysis of atmospheric NO_2 is due to radiant energy between approximately 3200Å and 4200Å. By utilizing the quantum efficiency for dissociation, the spectral absorption characteristics of NO_2, and the actinic irradiance, the rate constant for dissociation reaction of NO_2 in the atmosphere can be calculated. A value of 0.37 min^{-1} (0.0062 sec^{-1}) is accepted for typical clear atmospheric conditions[2].

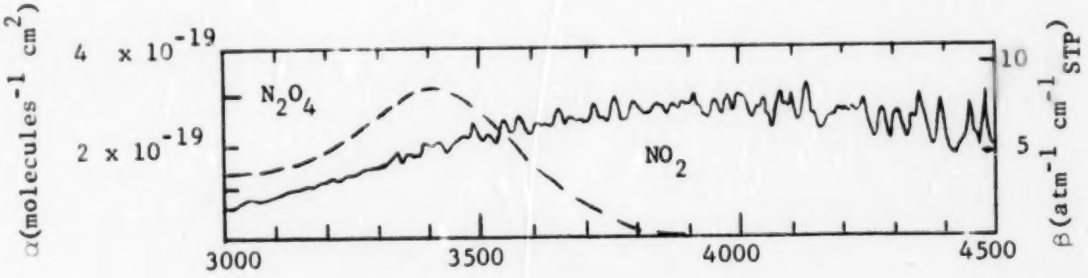

FIG. 1-1. Spectral plots of the absorption coefficient for NO_2 and N_2O_4 between 3000 cm^{-1} and 4500 Å. The ordinate scale shown on the right is convenient when the partial pressures of the gases are measured in atmospheres and the optical path lengths are in cm.

SECTION 2

PRELIMINARY TESTS

INSTRUMENTATION AND PROCEDURES

An optical diagram of the instrument used for the preliminary tests is shown in Fig. 2-1. The test bulb is filled with a mixture of NO_2 and O_2. Actinic radiant energy in the near uv and visible from lamp A causes a photochemical reaction that produces NO in the test bulb. The actinic energy can be blocked from the test bulb by shutter Sh. The remainder of the instrument is a gas-correlation cell analyzer that employs infrared energy to monitor the concentration of the NO in the test bulb.

Images of the radiant energy source are formed near the center of the test bulb and on the slit. A narrow beam of nearly-collimated energy is formed by the combination of the slit and the mask on the flat mirror near the source. After the beam passes through the slit, a rotating mirror chopper alternately directs it through one of two paths to a bandpass filter and detector. The 0.15μm wide bandpass of the filter centered near 5.3μm includes a portion of the strong, fundamental band of NO. Approximately 640 torr of NO in the 1 cm correlation cell is essentially opaque near the centers of the NO absorption lines and absorbs approximately 72% of the radiant energy in the bandpass of the filter. With no NO in the test bulb and with the blocking shutter B removed from the beam through the attenuator, the attenuator is adjusted so that the average transmittances of the two alternate beams are the same. Thus, the component of the detector signal at 170 Hz, the frequency of the rotating mirror chopper, is made zero.

When NO is formed in the test bulb, it absorbs a portion of the radiant energy leaving the detector. Because the NO in the test bulb absorbs

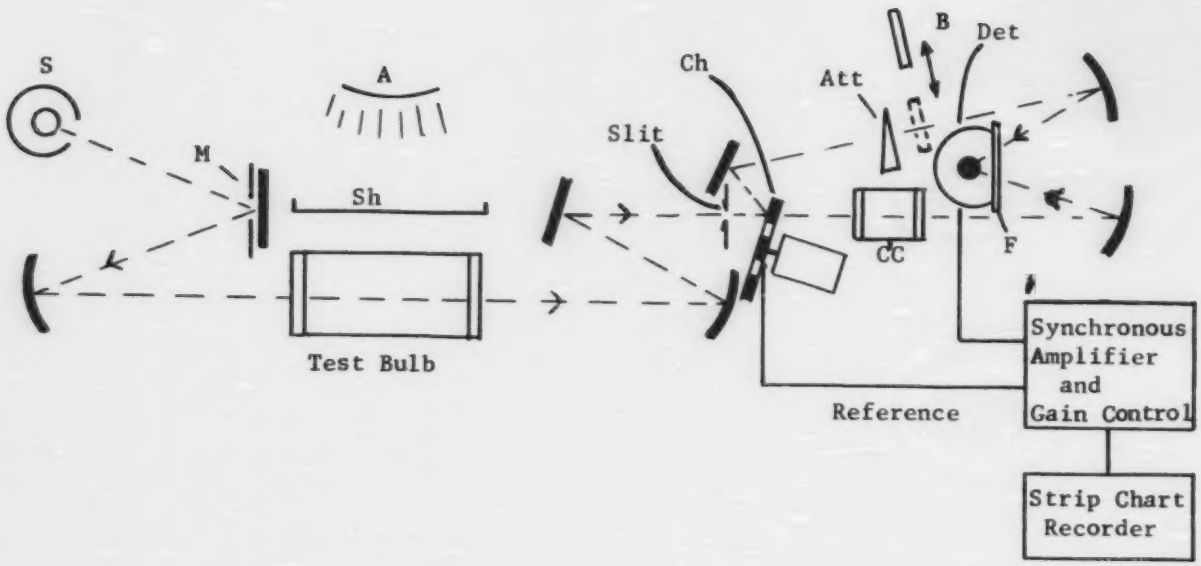

FIG. 2-1. Optical diagram of actinometer used for preliminary tests. S, infrared source. M, mask to limit IR beam size. Ch, chopper. CC, correlation cell containing NO. F, bandpass filter centered near 5.3 μm. Det, liquid-nitrogen cooled InSb detector. Att, adjustable attenuator. B, blocking shutter that can be moved into or out of the beam. A, source of uv and visible actinic energy. Sh, shutter to shade the test bulb from the actinic energy. When the instrument was used to investigate solar energy, the sky replaced A.

most at wavelengths where the NO in the correlation cell is opaque, the NO in the test bulb has less effect on the beam passing through the correlation cell than on the beam passing through the attenuator. The two alternate beams are no longer balanced and a detector signal at 170 Hz results. The percentage of misbalance between the two alternate beams is a measure of the concentration of NO in the test bulb. The spectroscopic principles of operation of gas cell correlation instruments have been described in detail in References 4 and 5.

In order to normalize the detector voltage, all of the NO is removed from the test bulb and the blocking shutter is moved so that it blocks the beam through the attenuator. The amplifier output for this condition is defined as V_b. The blocking shutter is removed from the beam and the attenuator is adjusted to produce zero amplifier output when no NO is present in the test bulb. As NO is formed in the test bulb, or introduced into it, a detector signal V_a results. The relationship between the ratio V_a/V_b and the amount of NO in the test bulb depends on the spectral bandpass as well as on the length of the correlation cell and the amount of NO in it. This ratio, V_a/V_b is defined as the normalized voltage V" and is nearly independent of source brightness or detector sensitivity provided neither of these parameters change after V_b has been measured.

A photoelectric pick-up produces an electric signal at the frequency of the mirror chopper and synchronized with it. This signal serves as a reference for the phase-lock amplifier (Princeton Applied Research Model JB-5). The amplifier output is recorded on a strip chart recorder. Electrical noise due to the detector and amplifiers is less than $10^{-4}V_b$ and does not contribute significantly to the uncertainty in the measurements.

The test bulb is cylindrical, 5 cm diameter by 10 cm long, with a quartz body and CaF_2 windows. Both the actinic source and the test bulb can be moved in a horizontal plane perpendicular to the narrow monitoring beam of infrared energy passing through the test bulb. Thus, the infrared beam can sample different portions of the test bulb to check for non-uniformity in the NO concentration. If mixing is not rapid, non-uniformities might be expected to result from gradients in the intensity of the actinic energy. For test bulb mixtures containing enough NO_2 that the absorption depth of the actinic energy is less than the diameter of the test bulb, the actinic energy density is less on the side of the test bulb away from the actinic source than it is on the opposite side. Reflection from the quartz wall can also produce non-uniform actinic energy density within the test bulb. For example, a line of high density may be expected along the cylindrical test bulb midway between the center and the wall farthest from the actinic source. Reflection of the nearly-parallel beam of actinic energy is focused along this line. By using a cylindrical test bulb, rather than a spherical one, it is possible to direct the infrared monitoring beam through a path parallel to the wall of the bulb and at different distances from it. Therefore, the actinic energy density is

nearly constant along the beam, and the effect of some of the geometrical factors contributing to non-uniform actinic energy density can be investigated more easily than with a spherical test bulb. Results obtained with the cylindrical test bulb have been used in determining the optimum diameter of a spherical test bulb and the $NO_2 + O_2$ mixture to be contained in it. The non-uniform directional sensitivity of the cylindrical test bulb does not create a serious problem for preliminary tests.

The irradiance by the artificial actinic source was approximately the same as that to be expected by solar energy near sea level on a typical clear day. Out-of-door measurements were made with the sun shining directly on the cylindrical test bulb and the artificial actinic source removed.

RESULTS OF PRELIMINARY TESTS WITH ACTINOMETER

An example of the recorder traces of the actinometer output during exposure of the test bulb to sunlight is given in Fig. 2-2. Before the trace was started, the test bulb had been shielded from actinic energy sufficiently long for all of the NO to disappear. At t = 0, the shutter was opened and the test bulb was exposed to sunlight; the increase in V" is due to the formation of NO in the test bulb. After approximately 2 minutes of exposure to the sun, the NO concentration was approaching equilibrium. A slight influence of a very thin cloud between the sun and the actinometer can be seen from about t = 2 to t = 5 min. At approximately t = 5 min., the intermittent shutter was turned on so that the test bulb was alternately dark for 30 seconds, then exposed to the sun for 30 seconds. We note that the amplitude, Δ", of the variation in V" due to the changes in NO associated with the intermittent shutter stabilized after only 1 or 2 minutes of intermittent exposure. Other data not shown indicate that the drift in the amplitude when the sky was clear was less than the drift in the steady-state value of V" when the shutter was left open for continuous exposure to the sun.

With artificial actinic energy from a "black light" source (Westinghouse H44-GS mercury vapor spot lamp) substituted for sunlight, responses such as those of Fig. 2-3 were obtained. At t = 0, there was essentially no NO in the test bulb because the shutter had been closed for several minutes to block the actinic energy. At about t = 2 min., the snutter was opened, exposing the test bulb to the artificial actinic source placed a distance D = 20 cm from the center of the test bulb. The shutter was then closed at about t = 6 min., and D was varied by moving the artificial source as indicated. The increased response after the shutter was re-opened resulted from the increase in irradiance associated with the decrease in D.

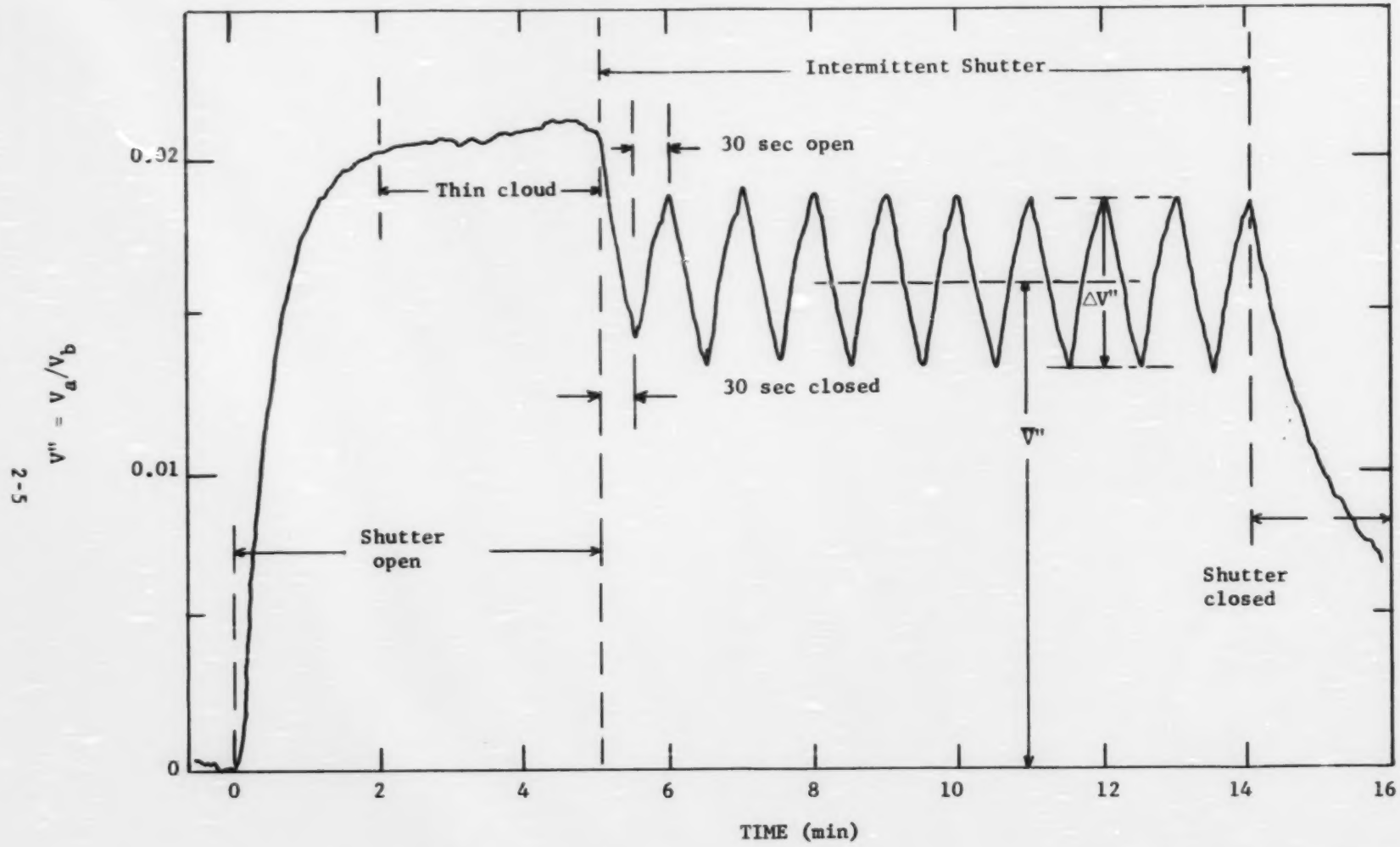

FIG. 2-2. Response of breadboard model NO_2 actinometer to sunlight. The test bulb was filled with 55 torr NO_2 plus 155 torr O_2. Exposure started at 12:29 P.M. (PDT) on June 29, 1973 near Newport Beach, Ca. at an elevation of approximately 50 m above sea level. The sky was mostly clear, but hazy with occasional thin clouds. The quantities $\Delta V''$ and $\bar{V}''$ for intermittent shutter operation are illustrated.

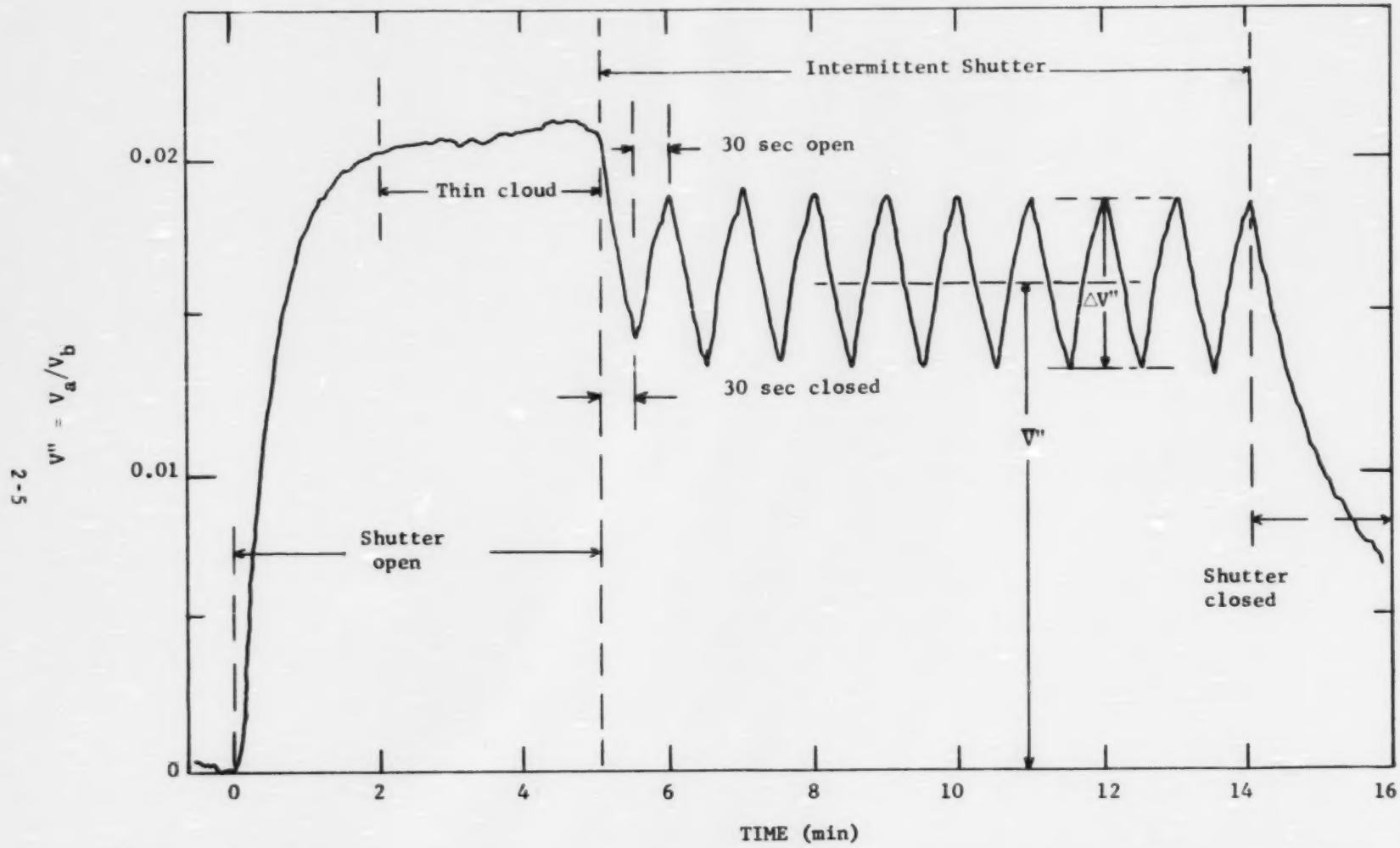

FIG. 2-2. Response of breadboard model NO_2 actinometer to sunlight. The test bulb was filled with 55 torr NO_2 plus 155 torr O_2. Exposure started at 12:29 P.M. (PDT) on June 29, 1973 near Newport Beach, Ca. at an elevation of approximately 50 m above sea level. The sky was mostly clear, but hazy with occasional thin clouds. The quantities $\Delta V''$ and $\overline{V}''$ for intermittent shutter operation are illustrated.

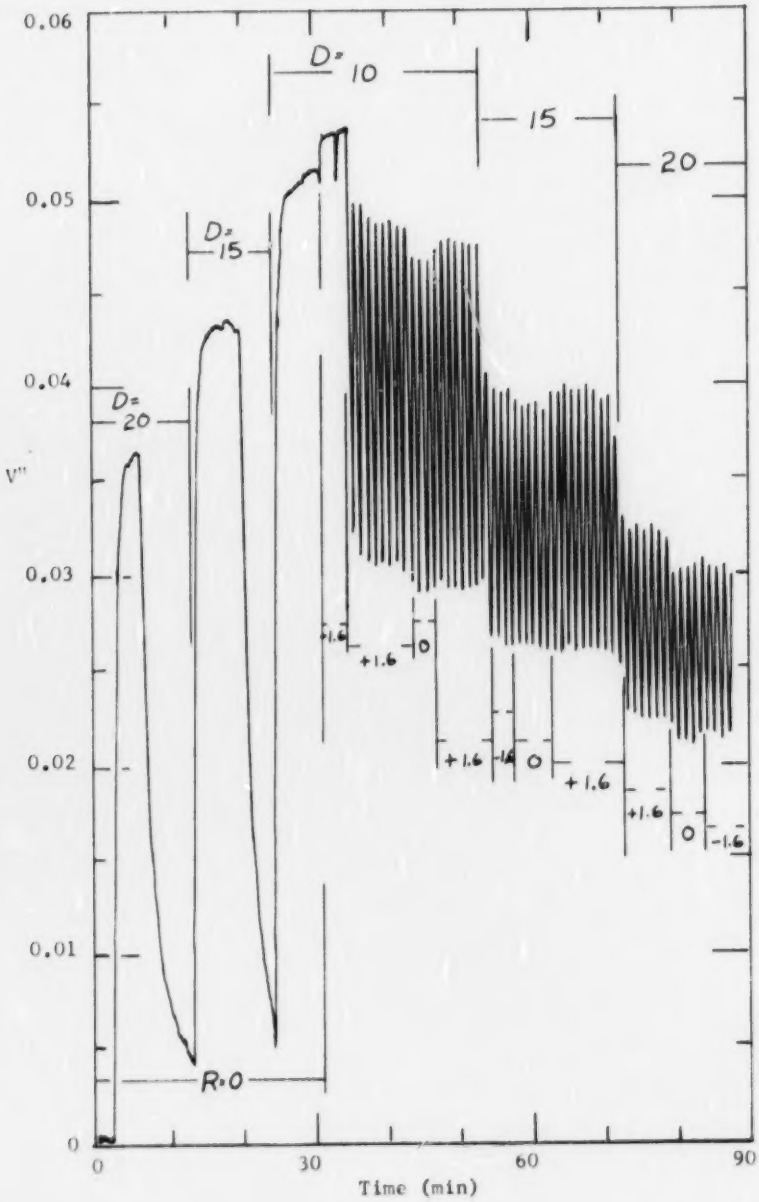

FIG. 2-3. Response of NO_2 actinometer to artificial uv and visible light at different intensities and different positions in the test bulb. D is the distance from the center of the test bulb to the face of the black light lamp used as the artificial actinic light source. The distance from the axis of the test bulb to the monitoring IR beam in cm is denoted by R; positive R indicates that the monitoring beam is between the axis of the test bulb and the actinic energy source, and negative R indicates that the monitoring beam is displaced in the opposite direction. The intermittent shutter is open 30 sec and closed 30 sec of each cycle. The test bulb was filled with 55 torr NO_2 plus 105 torr O_2.

At about t = 32 min., the actinic source and test bulb were moved as a unit relative to the IR monitoring beam to check for non-uniformities in the NO concentration in the test bulb. The apparent shift in response when the test bulb was moved is due primarily to a "zero" shift arising from non-uniformity in the CaF_2 windows on the test bulb. The amount of zero shift due to the windows was measured with the test bulb evacuated. After the shift was accounted for, the results indicated there was no significant difference in the NO concentration at the three different positions of the test bulb for the NO_2 and O_2 mixture given in the legend of Fig. 2-3. When the intermittent shutter was used, the amplitude $\Delta V''$ was also essentially the same at all three values of R when D remained fixed. This provides additional evidence that the NO is mixed under these conditions.

Similar tests for non-uniform NO concentrations were also made with higher and lower pressures of NO_2 and O_2 in the test bulb. With NO_2 pressures greater than approximately 100 torr and O_2 pressures greater than approximately 150 torr, there was evidence that the NO concentration was higher on the side of the test bulb toward the actinic light source. At the higher NO_2 pressures, a large fraction of the actinic energy is absorbed and forms NO before it has penetrated through the cell. The higher pressure also reduces the mixing rate in the test bulb. Thus, there are upper limits on the pressures of NO_2 and O_2 that can be used in a spherical test bulb of a field instrument in order that the concentration along the diametric path of the monitoring beam represent the average for the entire bulb. This is required if the response is to be independent of the direction of the incident actinic energy.

From Fig. 2-3 we see that the steady-state values of V" obtained with the shutter open and the amplitude $\Delta V''$ of this quantity when the shutter is intermittent both increase as the actinic irradiance is increased by decreasing D. The dependence of both V" and $\Delta V''$ on the actinic irradiance are shown in Fig. 2-4 for the conditions represented by Fig. 2-3. The relative irradiances were measured with the probe of a "lite-Mike" (EG&G, Inc. Model 560B) at the normal position of the center of the test bulb. The steady state value of V" tends to saturate at much lower actinic irradiance than does $\Delta V''$ obtained with the intermittent shutter. A near-linear relationship exists between V" and the actinic irradiance over a wide range of irradiance values.

Figure 2-5 illustrates the dependence of the actinometer response on the partial pressures of NO_2 and O_2. Values of $\Delta V''$ increase nearly in proportion to the P_{NO_2} with little or no O_2 in the test bulb. Adding O_2 to a fixed amount of NO_2 increases the amplitude ΔV because it increases the rate at which the NO returns to NO_2 during the dark half of each cycle. In the upper panel, the plot of V" for P_{NO_2} = 72 torr illustrates the decrease in the equilibrium amount of NO with increasing O_2 when the test

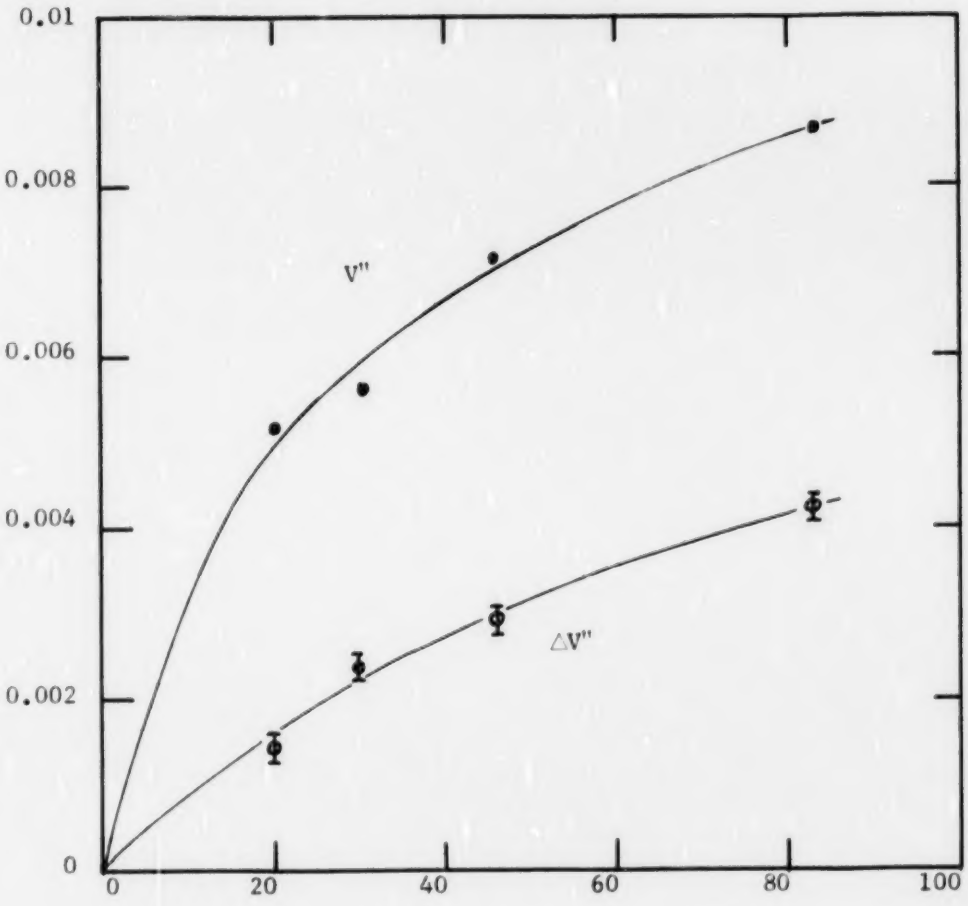

FIG. 2-4. Plots of V" and ΔV" vs relative actinic irradiance. The ordinate for each curve is labelled.

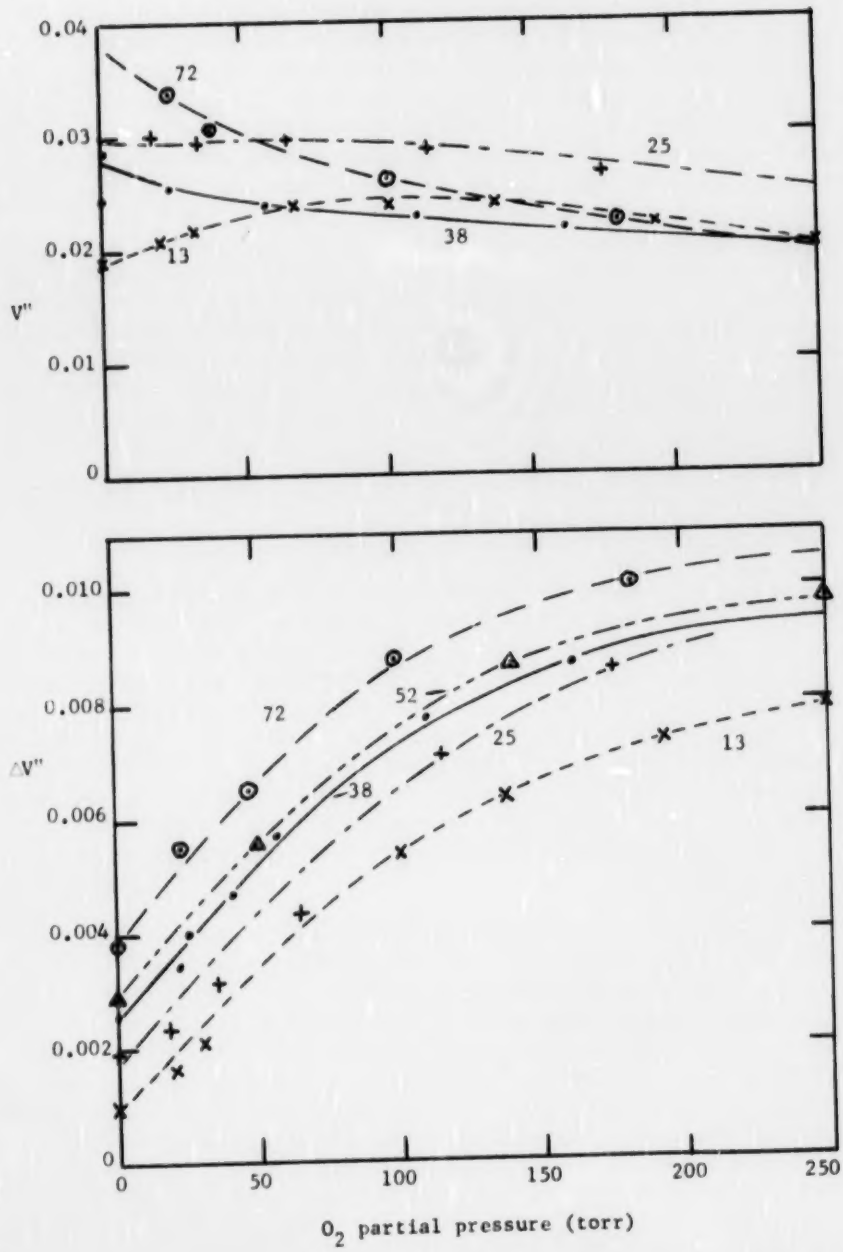

FIG. 2-5. Plots of V" and ΔV" vs O_2 partial pressure in the test bulb for various partial pressures of NO_2. The partial pressures of NO_2 in torr are indicated for each curve. A uv black light without a filter served as the source of actinic energy. The monitoring beam passed along the center of the 10 cm long test bulb. While measuring ΔV", each shutter cycle consisted of periods of 30 sec open and 30 sec closed; V" was measured after the shutter had been open several minutes.

bulb is irradiated continuously. This result is to be expected because of the increase in the rate of the reverse reaction producted by the additional O_2. The measurements of V" for the lower values of P_{NO_2} were not reproducible and were inconclusive. Variations in temperature and the amounts of impurities in the test bulb probably account for the changes in V" while the actinic irradiance is maintained constant. These variations apparently have less influence on ΔV" than on V".

Increasing the pressure of either NO_2 or O_2 increases ΔV"; however, as pointed out above, if the pressures are too high the actinic energy density and the NO concentration are not uniform throughout the test bulb, and the interference by N_2O_4 is significant. The optimum pressures for a test bulb of a given diameter in a field instrument are determined by the best compromise among the spectral response, uniform directional response, and signal-to-noise ratio. Therefore, the optimum pressures depend upon the detectivity of the detector and the radiance of the IR source and can best be determined after an instrument is assembled. Decreasing the O_2 pressure increases the required period for the shutter because of the decrease in the rate at which the NO disappears during the dark portion of the cycle.

A few tests were made on the influence of temperature changes in the test bulb while maintaining the amount of gas in it and the actinic irradiance constant. An infrared heat lamp heated the test bulb, and a thermocouple, inserted into the interior of the bulb but shielded from the direct radiation of the heat lamp, measured the temperature of the gas in the bulb. For a typical gas mixture, ΔV" increased by approximately 9% as the temperature changed from 300 K to 320 K; an additional 20 K increase produced an additional 5% increase in V". The value of ΔV" quickly stabilized after the temperature had been changed. Steady-state values of V" obtained with the shutter open were more dependent on temperature and much less stable than those of ΔV".

We have performed other tests on NO detection in our laboratory with a gas cell correlation instrument employing the same bandpass filter and correlation cell as those illustrated in Fig. 2-1. Absorption by water vapor in the atmospheric path in the instrument interferes with the NO measurement and produces a shift in the zero reading that corresponds to the test bulb being free of any NO. If the H_2O concentration is constant it can be accounted for by adjusting the zero setting when the test bulb has been shaded from actinic energy sufficiently long for all of the NO to disappear. However, variations in the H_2O concentration can cause zero shifts that produce significant errors in measurements of V". Errors in ΔV" produced by H_2O interference are much smaller because this quantity represents the decrease or increase in V" each time the shutter is closed or opened. If several measurements are repeated, the errors cancel each other out.

Results obtained in the sunlight with a test bulb having a borosilicate glass body were similar to those obtained with a test bulb made of quartz, which is known to be transparent in the spectral interval of the actinic energy. Although the glass is known to absorb strongly at the shorter wavelengths of the actinic energy, values of $\Delta V''$ were only about 10% less for the glass test bulb than for the quartz one. A greater difference might be observed where shorter wavelengths comprise a greater proportion of the actinic energy than that transmitted through the hazy atmosphere of these tests.

MONITORING OF NO_2 VS NO

Nitrogen dioxide has at least three absorption bands[6] in the infrared and visible that are worthy of consideration for a gas cell correlation instrument designed to monitor this gas. The strongest infrared band near 6.2 μm is probably not practical for an instrument with a significant optical path in the atmosphere because of excessive interference by the strong, overlapping H_2O absorption. Furthermore, no convenient detector with adequate detectivity without cryogenic cooling exists for this band. Considerable structure exists in the spectrum of the 3.4 μm band so that it lends itself to the use of gas cell correlation techniques. This band is also relatively free of interfering absorption by H_2O or other atmospheric gases. However, its band strength is only moderate so that the sensitivity of an instrument employing this band is limited. A relatively convenient detector with a thermoelectrically cooled PbSe element would probably be adequate for the 3.4 μm region.

As pointed out in Section 1, most of the NO_2 absorption in the uv is continuous without enough structure in the spectrum for a gas cell correlation instrument to operate efficiently. We have investigated the use of the absorption features in the visible spectrum. These features are quite distinct and consist of many very closely spaced lines that overlap except for very low sample pressures. Fig. 2-6 shows spectral curves of transmittance obtained with a spectral slitwidth of approximately 2 Å. Absorption is quite strong, even at wavelengths adjacent to the stronger absorption features. Thus, the strong absorption features are not separated by narrow regions of little or no absorption as are the lines in the fundamental NO band near 5.4 μm. Because of the absorption between the wavelengths of strongest NO_2 absorption, a gas cell correlation instrument is less efficient than we had originally expected. Our tests on these visible NO_2 bands were limited to the measurement of NO_2 in a conventional absorption cell, rather than in a test bulb with NO_2 being dissociated photochemically.

We have used the actinometer illustrated in Fig. 2-1 to obtain data such as those represented by Fig. 2-2 as well as to study stable samples of $NO + N_2$ in the test bulb. By comparing the results, we have been able

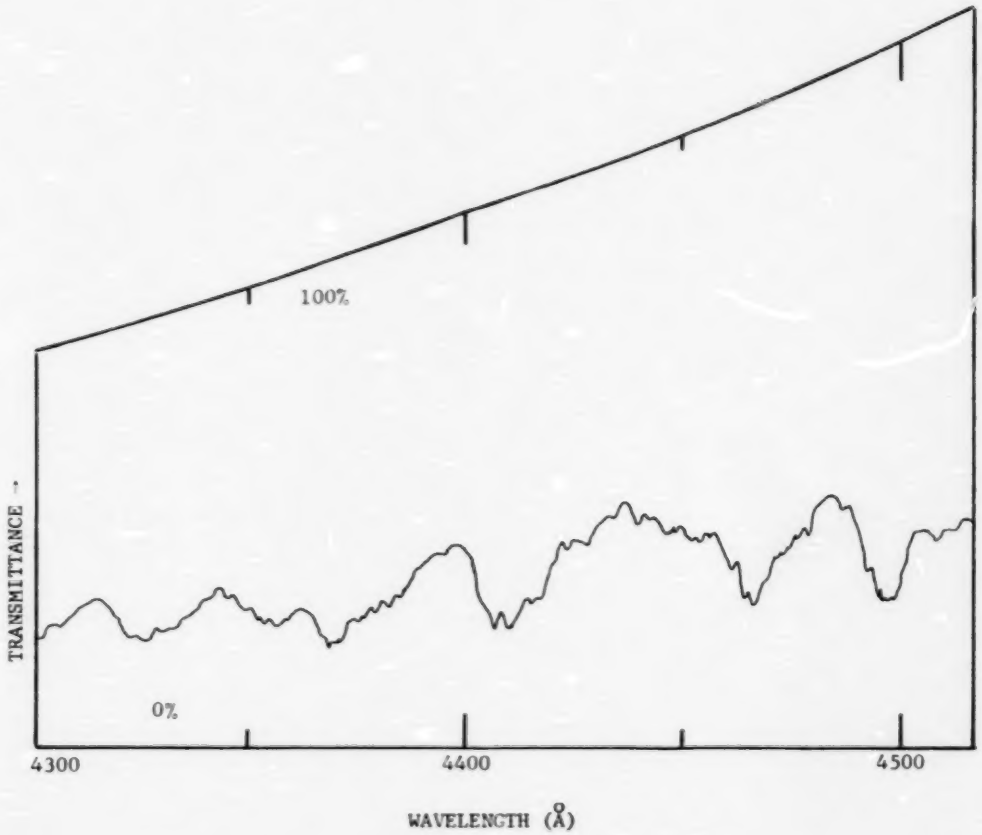

FIG. 2-6. Transmittance of NO_2 from 4300 to 4500 Å. The sample cell length was 3.96 cm, the pressure of NO_2 was 25 torr, and the temperature was 51°C.

to estimate the NO concentration in the test bulb from the measurement of V". During the period when the shutter was cycling to obtain the data shown in Fig. 2-2, the concentration of NO was oscillating from about 4% to 6% of that of the NO_2. It follows that the NO_2 concentration was varying from approximately 94% to 96% of its original value. If the actinometer were made to measure the NO_2 concentration, rather than NO, it would be required to measure the small relative change quite accurately. Because the relative change in the NO concentration is much greater, the required accuracy for its measurement is much less. For example, the temperature of the test bulb can be expected to oscillate slightly in synchronism with the opening and closing of the shutter over the test bulb. The small temperature change can influence slightly the absorption characteristics of both the NO_2 and the NO and produce an error in the measurement of $\Delta V"$. Such an error would be more serious when measuring the small relative changes in NO_2 than when measuring the larger relative changes in NO.

After considering the encouraging results obtained with the actinometer measuring NO concentrations and the problems anticipated in measuring the changes in NO_2 concentrations, we decided to build the final instrument to measure the changes in NO.

HOT NO AS AN IR ENERGY SOURCE

The use of a hot gas cell containing NO as a source of infrared energy in place of a conventional continuous source has been considered, and a few related experiments have been performed. Such a source would provide the energy for the monitoring beam in an actinometer that monitored the formation of NO in the test bulb. The hot NO in the source cell emits strongly near the centers of the absorption lines which, of course, are at the wavelengths of strong absorption by the NO in the correlation cell and in the test bulb. The length, L, of the hot source cell and the pressure P_{NO}, of NO in it should be adjusted so that the product $L\ P_{NO}$ is somewhat greater than the corresponding quantity for the NO in the correlation cell. On the other hand, it should be small enough that there is not appreciable emission at wavelengths midway between adjacent lines.

Little information about NO in the test bulb can be obtained from the wavelengths well separated from the line centers. Therefore, the extra energy emitted by a continuous source at these wavelengths produces little information, but it can contribute to misbalance, drift and interference by other gases that may be present in the optical path. Because of the coincidence of the emission lines of the source gas and the absorption lines of the absorbing gas in the test bulb, a fixed amount of absorbing gas absorbs a larger fraction of energy from the hot gas source than from a continuous source. For a low concentration C of NO in the test bulb of optical path length L_{TB}, the normalized voltage V" is related to C by

$$V'' = V_a/V_b = k\ C\ L_{TB}. \qquad (2\text{-}1)$$

It follows from the above discussion that the constant k can be larger when using a hot NO source than when using a continuous source. Thus a given percentage error in balance of the instrument yields a smaller error in the measurement of C when using the hot NO source.

Hot gas cells generally cannot be operated at temperatures as high as continuous sources, with the result that both V_a and V_b are lower for hot gas sources. In the case that the instrument accuracy is limited primarily by detector noise, the increased energy available from the continuous source makes it preferable to the hot gas source. The results of the tests made with the actinometer shown in Fig. 2-1 indicated that the larger values of k and the better discrimination available with the hot NO source would not be as important for the actinometer to be built as would the extra signal available with the continuous source. The extra signal is required because it is desirable that the actinometer not require a cryogenically-cooled detector; therefore, the detector detectivity is much lower than that of the liquid nitrogen-cooled detector used in the preliminary tests.

CONCLUSIONS DRAWN FROM PRELIMINARY TESTS

The results of the tests reported here indicate the feasibility of an NO_2 actinometer for field use in which the concentration of photochemically-produced NO is monitored by non-dispersive infrared techniques. Accurate steady-state values of NO concentration are difficult to determine because of instabilities in the optical components and variations in the temperature of the test bulb. Other slow chemical reactions not considered here may also produce slow changes in the NO concentration. In contrast, results that are more consistent and easier to interpret can be obtained by using alternate light and dark periods of approximately 30 to 60 seconds each to produce rapid changes of NO concentration around a mean level. The alternating method has the problem that the total response is reduced substantially and the cycle periods must be controlled carefully. However, these problems are more than offset by the improved stability. The relatively slow response in both methods precludes the measurement of small, rapid fluctuations of the actinic light level. Monitoring the concentration of NO can apparently provide a more accurate measure of the actinic energy than is possible by monitoring the NO_2.

Although the optimum instrument parameters depend on a variety of operating conditions, it is possible to prescribe approximate parameters for a potentially useful tool for measuring the relative available actinic light under most natural conditions of interest. A spherical, quartz test bulb 10 cm in diameter filled with a mixture of $NO_2 + O_2$ can be made

with its sensitivity to light nearly the same from all directions in the upper hemisphere. The amount of NO produced under normal atmospheric conditions is sufficient to be measured by non-dispersive infrared techniques employing a gas correlation cell. The addition of an inert gas such as N_2 to the mixture in the test bulb is not required and would reduce the rate of mixing of the gases and increase non-uniformities in the NO concentration.

A small, readily available InSb detector with thermoelectric cooling to about 250 K can probably provide an adequate signal-to-noise ratio when used with a conventional infrared energy source. Cooling the detector to lower temperatures with liquid nitrogen is probably not required. The advantage of improved discrimination that could be achieved by using hot NO as the infrared source is more than offset by the increased complexity and decrease in signal.

Windows on the test bulb for the transmission of the IR monitoring beam and associated mirrors necessarily decrease the sensitivity of the system to actinic light arriving from certain directions. By properly orienting the test bulb relative to the sun so that the windows and mirrors do not interfere with the direct sunlight, it is possible to minimize the error caused by these interfering optical components.

SECTION 3

DESCRIPTION OF ACTINOMETER

OPTICAL LAYOUT

The requirements described above and the results of the preliminary tests described in Section 2 led to the design and construction of the instrument illustrated in Figs. 3-1, 3-2 and 3-3. The upper panel of Fig. 3-1 shows an optical schematic diagram as viewed from above. Infrared radiant energy is directed by mirror M1 through a correlation cell with an image of the source formed at the reflecting plane of the mirror chopper. When the notched, mirror chopper is in the open position, the beam continues on and another image of the source is formed on the small, flat mirror, M8, which is tilted approximately 22.5° from the vertical so that the beam is reflected at 45° upward to mirror M9, which returns the beam displaced slightly sidewise to a CaF_2 lens. A reduced image of the source is formed on the detector.

During the other half of each cycle the mirror chopper, the energy falling on the detector is directed by mirror M3 through an attenuator to the reflecting surface of the mirror chopper. The fixed portion of the attenuator is a sapphire window, and the adjustable portion blocks a portion of the beam. Beyond the mirror chopper, the beam travels the same path during both halves of the cycle. Mirror M8 is sufficiently short that it limits the useful length of the source from which radiant energy is collected. Spherical mirror M7 images mirror M6 near mirror M9, which is bonded to the quartz test bulb and forms the aperture stop. The mask on mirror M6 reduces scattered light that would not be collected by M9. A narrow bandpass filter similar to the one shown in Fig. 2-1 is placed in front of the detector and limits the spectral band to a region approximately 0.15 microns wide centered near 5.3 microns.

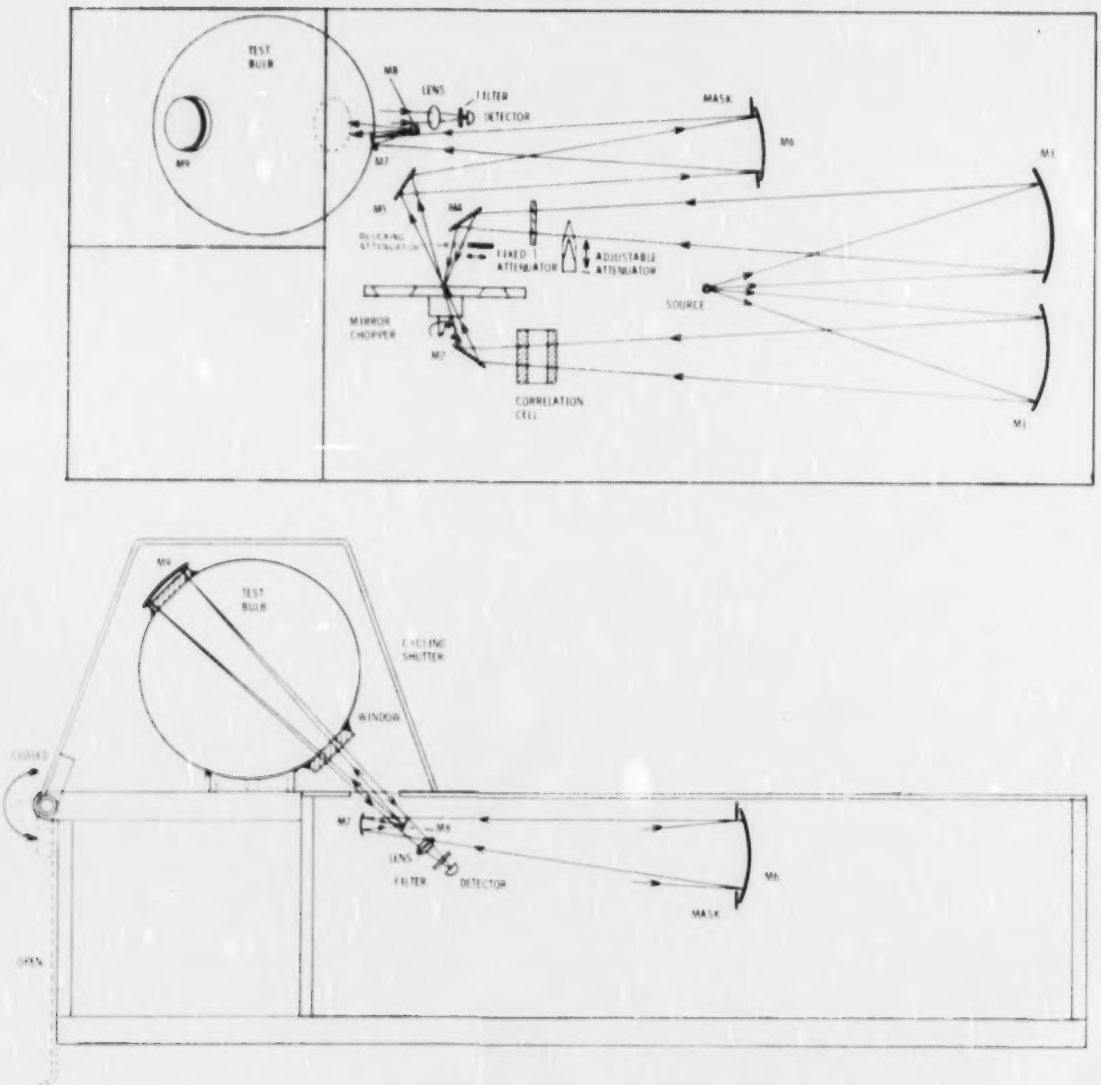

Fig. 3-1. Optical diagrams of the optics assembly of the actinometer. The upper panel is a top view with the instrument in its normal operating position. A side view of a portion of the instrument is shown in the lower panel.

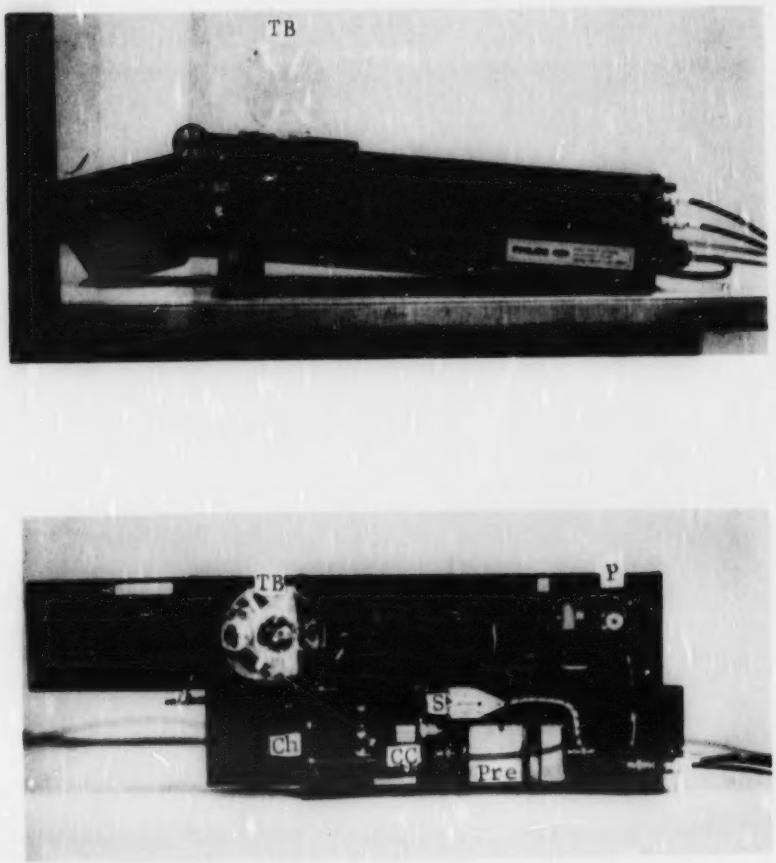

FIG. 3-2. Two views of the optics assembly of the actinometer. The upper panel shows the instrument completely assembled with the shutter open. The lower panel shows a top view with the shutter open and the lid removed. S, source; CC, correlation cell; Ch, mirror chopper; TB, test bulb; Pre, preamp.; P, power supply.

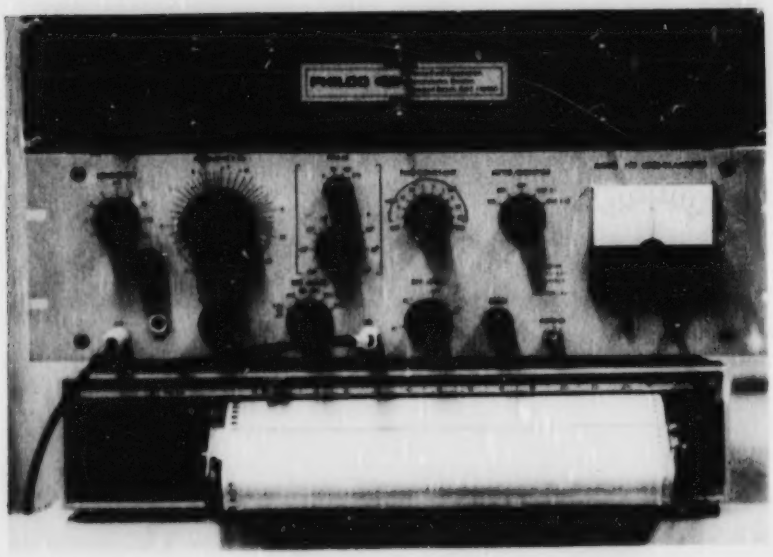

FIG. 3-3. Photograph of the control assembly, amplifier and recorder. The control assembly contains switches and a timer assembly for remote control of the shutter and the recorder.

Approximately 10 torr of NO_2 plus 110 torr of O_2 has been added to the quartz test bulb. As the test bulb is irradiated with actinic energy, from the sun or from an artificial source, part of the NO_2 is photolyzed to produce NO and O_2 according to Eq. (1-1). The shutter periodically covers the quartz test bulb to shade it from actinic energy. Out of each 2 min period of the shutter, it is open approximately 55 sec and closed for 55 sec. Approximately 5 sec are required for the shutter to open or close. The primary purpose of the instrument is to measure the change in the concentration of NO in the test bulb during the two halves of the shutter cycle.

The spectroscopic principles of operation of this instrument are the same as those of the breadboard instrument shown in Fig. 2-1. After the shutter has been closed sufficiently long that essentially all of the NO has disappeared from the test bulb, the attenuator is adjusted so that the same amount of infrared energy is incident on the detector during both halves of cycle of the mirror chopper. Thus, there is no detector signal at 350 Hz, the chopper frequency. The adjustable attenuator is mounted directly to a micrometer screw and is moved into or out of the beam. After the instrument has been balanced, the quantity V_b is measured by moving the blocking attenuator to the position indicated by the broken line in the upper panel of Fig. 3-1. This blocks all of the energy that normally passes through the attenuator with the result that the infrared energy reaching the detector is completely modulated by the mirror chopper. After the quantity V_b has been measured and recorded, the blocking attenuator is moved to its normal position before measurements are made.

DESCRIPTION OF OPTICAL AND MECHANICAL COMPONENTS

The source is a ceramic-coated resistance wire that is heated electrically by approximately 10 amperes of alternating current at 2.5 V. This source is commercially available from Perkin-Elmer Corporation and receives power from a small transformer. Its spectral radiance in the region of interest, near 5.3 microns, is only approximately half that of a Nernst glower under normal operating conditions. However, this source is easier to operate, and its durability makes it more practical for a field instrument.

The mirror chopper is machined from stainless steel and has 6 reflecting blades and 6 openings of equal width. The reflecting surface has been coated with a thin layer of aluminum and polished to produce good reflectivity. The chopper is mounted directly to the shaft of a small induction motor that rotates at approximately 3500 rpm to produce a chopping frequency near 350 Hz. This frequency is sufficiently high that the detectivity of the detector is not seriously limited by the 1/f noise. In order to obtain higher chopper frequencies, either more blades would be required on the chopper or it would need to be rotated at a higher frequency. Either of these methods has obvious disadvantages.

The detector contains a 2 mm x 2 mm sensitive element of InSb that is cooled to approximately -25°C by a small thermo-electric cooler that receives its power from a dc power supply mounted in the position shown in Fig. 3-2. A separate supply powers the preamplifier and the reference pick-up and produces bias voltage for the detector.

Calcium fluoride windows are sealed by epoxy cement to the 1 cm long by 2.5 cm diameter correlation cell. Approximately 680 torr of NO in the correlation has an average transmittance of 72% in the spectral band of the bandpass filter.

The test bulb is approximately 10 cm in diameter and is made from the spherical bulb of a quartz beaker. Holes approximately 2.2 cm in diameter have been cut in the walls; CaF_2 windows are bonded with epoxy cement over the holes. The quartz wall had to be removed from the windows because quartz is opaque to the 5.3 micron infrared energy in the monitoring beam. A piece of Monel tubing has been bonded in a smaller hole cut in the bottom of the test bulb. A small Monel valve welded to the tubing makes it possible to evacuate the test bulb and refill it with any desired mixture at a pressure less than 1 atm. It is anticipated that the mixture of NO_2 + O_2 in the test bulb can be used for several months without refilling.

The test bulb is mounted above the remainder of the instrument in order that it can receive actinic energy from as much of the upper hemisphere as possible. It seems likely that a negligible portion of actinic energy would be reflected from the earth's surface. Thus, most of it would be incident on the test bulb from a direction above the horizon. Ideally, the bulb should have no obstruction that would shade any part of it from any part of the upper hemisphere. However, it is necessary to obstruct small portions of the test bulb in order to pass the infrared monitoring beam across a diameter. The CaF_2 window on the lower side of the test bulb is not expected to obstruct a significant portion of the actinic energy from the sky. The window and mirror M9 on the upper portion of the test bulb probably cause the most obstruction and produce the biggest deviation in the sensitivity from all directions. On most days, it is expected that a large fraction of the actinic energy will come from a direction within several degrees of the sun. Therefore, the influence of the windows and mirror M9 can be minimized by orienting the instrument so that these parts produce a minimum of obstruction of light coming directly from the sun. This is best accomplished by locating the instrument with the end containing mirrors M1 and M3 pointed in the azimuthal direction of the sun. Unless the sun is very high in the sky, shading by mirror M9 should not be serious. It seems likely that the shading of the test bulb by the windows and the mirror is less under most circumstances when oriented in this manner than would be possible if mirror M9 were located on the top of the bulb with the monitoring beam

traveling along a vertical diameter. Double passing the test bulb with the infrared monitoring beam increases the sensitivity of the system without enlarging the diameter of the test bulb. Although mirror M9 shades part of the test bulb, removing it so the beam single-passes the test bulb would not significantly decrease the shading because another mirror would need to be placed near the bulb to direct the beam to the detector.

In order to further minimize any obstruction of the test bulb from light in the upper hemisphere, the legs on the instrument are made so that it slopes downward at about 5° from the test bulb toward the end containing mirrors M1 and M3. The shutter, when open, also is below the horizon from any point on the test bulb.

The cycling shutter is chain driven by a small gear motor that is turned on and off and reversed in direction by a timing mechanism mounted in the control panel described below. Microswitches actuated by the shutter turn the motor off as it approaches either the closed or open position. A small slip-clutch mounted to the shaft of the motor allows the shaft of the gear motor to continue turning for a short time after the power has been turned off and the shutter has reached the end of its travel. It is necessary to allow for this small amount of slippage because of the angular momentum of the armature of the motor.

Fig. 3-3 shows the control unit, the synchronous amplifier, and the strip chart recorder. On-off switches on the front panel of the control assembly operate the chopper, the source, and the detector. When the shutter-control switch is in the manual position, the shutter can be either opened or closed by holding a spring-loaded switch in the appropriate position. The automatic timer controls the action of the shutter when the shutter-control switch is in the automatic position. If no electrical power is available, the shutter can be opened or closed by forcing it slowly and allowing the clutch to slip.

When the chart recorder-control switch is in the manual position, the pen remains in the writing position and the chart is controlled by the switch on the front of the recorder. With the chart recorder-control switch in the automatic position, both the chart drive and the pen may be deactivated by the timer. In the automatic mode, the chart drives and the pen writes only for two intervals of about 10 seconds each during each shutter cycle when V" is near its minimum and maximum values. By recording only during these intervals, the amplitude that corresponds to $\Delta V"$ can be measured easily and less chart paper is required. Recorder tracings that illustrate the use of the chart recorder in the automatic mode appear in Section 4. The period of time that the pen writes on the strip chart can be changed by adjusting the appropriate cams in the timer assembly.

A push-button switch on the front panel of the control unit actuates an "event-marker" pen that records on the right-hand side of the strip chart. The electrical cables that connect the optics assembly to the control unit, recorder, and amplifier are approximately 8 meters long and can be removed for easy handling. Detailed wiring diagrams are shown in Section 5.

SET-UP AND OPERATION

The instrument is designed for use in the position shown in the upper portion of Fig. 3-2. The bench or table on which it is placed should be small so that it subtends a small solid angle from the test bulb and thus blocks a minimum of actinic energy. Other structures that block actinic energy from the bulb should also be avoided. As pointed out previously, the amount of energy blocked by mirror M9 on the test bulb is minimized by orienting the instrument so that the right-hand end in Fig. 3-2 is in the azimuthal direction of the sun. The outside surface is blackened to minimize reflection of actinic energy to the test bulb.

The power supplies and the source produce enough heat inside the instrument cover to increase the temperature by several degrees. Overheating of the power supply for the detector coolers is avoided by heat-sinking it to one side of the box. It is recommended that a fan be used to circulate air over the optics assembly to reduce its temperature, particularly if it is being used in hot, sunny weather or in a hot test chamber. Increased temperature degrades the signal-to-noise ratio of the cooled detector. Excessive temperature changes in the test bulb also change the response of the instrument.

All of the electrical plugs and connectors are labeled so that the instrument can easily be connected in accordance with Fig. 5-2. A few minutes should be allowed for warm-up before the following adjustments are made. The beam in the attenuator side of the alternator is blocked by moving the knob for the blocking attenuator to the BLOCK position. The knob is located near the chain-drive for the shutter. Adjustments are then made to the amplifier frequency and phase to produce a maximum positive output of the amplifier. The amplifier frequency reading should be approximately 350 Hz, the chopper frequency. Positive output corresponds to a reading to the right of center on the meter on the amplifier panel with the meter-monitor switch in the OUT x 1 or OUT x 10 position.

Zero and span adjustments on the amplifier and recorder are made in the following manner. Set the meter-monitor switch to the OUT x 10 position and disconnect the signal input cable to the amplifier. Use the zero adjustment on the amplifier to set the meter reading to zero (center). Next, adjust the recorder zero potentiometer on the front panel of the recorder to produce a zero reading of the recorder. Set the meter-monitor

switch on the amplifier to the OUT x 1 position and rotate the zero-adjustment potentiometer on the amplifier clockwise until the panel meter reads full-scale (10) to the right. Now, use the recorder-adjust potentiometer on the rear of the amplifier to produce a full-scale reading of the recorder. Return the zero-adjustment potentiometer of the amplifier to the position that produces a zero, or mid-scale, reading on the meter. Reconnect the signal input cable to the amplifier. The recorder is now spanned so that a full-scale reading corresponds to full-scale of the amplifier panel meter and is within the useful dynamic range of the amplifier. A 1 K ohm resistor across the input terminals of the recorder matches the recorder to the amplifier output. A zero off-set of the recorder can be obtained by adjusting the zero-potentiometer on the recorder.

In normal operation, the chart speed-control switches on the recorder and on the control assembly are in the LO position. When the control switch of the control assembly is in the FAST position, the chart speed is opposite to that indicated by the switch on the recorder. The chart speed-control switch on the control assembly is not needed but was installed before the recorder was delivered.

From Section 2, we recall that the instrument output of interest is $\Delta V"$, which is proportional to $\Delta V/V_b$, where V_b is the output with the attenuator leg of the alternator blocked, and ΔV is the change in the output as the shutter periodically opens and closes. (See Fig. 2.2.) Before starting a series of measurements, the blocking attenuator is moved to the BLOCK position to block the beam in the attenuator leg and V_b is measured. At the time the instrument was delivered to EPA, V_b corresponded to a recorder-pen of approximately 17 cm with the amplifier on 20 mv scale. In order to simplify the conversion of ΔV to $\Delta V"$, the pen deflection can be adjusted to produce an even-numbered deflection, such as 20 cm. This is done by adjusting the calibration-potentiometer on the input of the amplifier. It is best if this is done after the shutter has been closed sufficiently long that little NO remains in the test bulb.

After V_b has been measured and recorded, the blocking attenuator is removed from the beam and the alternator is balanced with the adjustable attenuator while the shutter is kept closed to avoid the formation of NO in the test bulb. The instrument is then ready for operationin the manner described previously. Ordinarily, the system is balanced with the amplifier on a more sensitive scale, either 1 mv or 2 mv full-scale. Measurements of ΔV are also made on the most sensitive scale. In relating the pen deflections to V" or $\Delta V"$, the different sensitivities of the amplifier must be accounted for. For example, assume that a recorder-pen deflection of 20 cm was observed when measuring V_b with the amplifier on the 20 mv scale. When the actinic irradiance is being measured, the amplifier is on the 1 mv scale. As the shutter opens and closes during

its cycle, the pen deflection varies from a maximum of 13 cm to a minimum of 9 cm, giving a difference of 4 cm. If V_b had been measured on this scale, it would have corresponded to a pen deflection of 20 x 20/1 = 400 cm. Therefore, $\Delta V'' = 4/400 = 0.010$.

After several minutes of warm-up, V_b remains nearly constant for several hours unless the instrument temperature changes significantly. Thus, the frequency that V_b needs to be checked depends on the weather conditions if the instrument is outside, or upon the temperature in a test chamber.

SECTION 4

TEST RESULTS AND INSTRUMENT PERFORMANCE

RESPONSE TO SOLAR ENERGY

The recorder tracing shown in Fig. 4-1 illustrates the actinometer output in the afternoon of a clear day in early June in Newport Beach, California. The instrument was located on a roof top with essentially clear vision above the horizon in all directions. Before time t = 0, the actinometer had been balanced with the shutter closed so that no NO was present in the test bulb. At t = 0, the shutter was opened; thereafter the chart drive and the pen operated continuously while the shutter opened and closed with a two-minute period. At t = 0, 2, 4, 6 --- minutes the shutter opened; it closed at t = 1, 3, 5, 7 --- minutes. While the shutter was open, V" did not increase linearly with time during the full one-minute period. This non-linearity contributes significantly to the non-linear relationship between $\Delta V"$ and actinic irradiance.

The first peak is not as high as the following ones because the NO concentration had not reached its maximum value when the shutter closed at t = 1 minute. After two cycles of opening and closing the NO concentration has essentially reached the point so that the maximum and minimum values of V" repeat themselves if the actinic irradiance is constant. Typically, the maximum value of V" attained during cyclic operation of the shutter is between 2½ and 3 times $\Delta V"$, the difference between the maximum and minimum values of V". Detector noise is the major cause of small, high-frequency variations in V". The peak-to-peak noise equivalent V" is typically less than 0.001 with an amplifier time constant of 1 second.

Recorder tracings of the actinometer output are shown in the upper panel of Fig. 4-2 for both the recorder and shutter operating in the

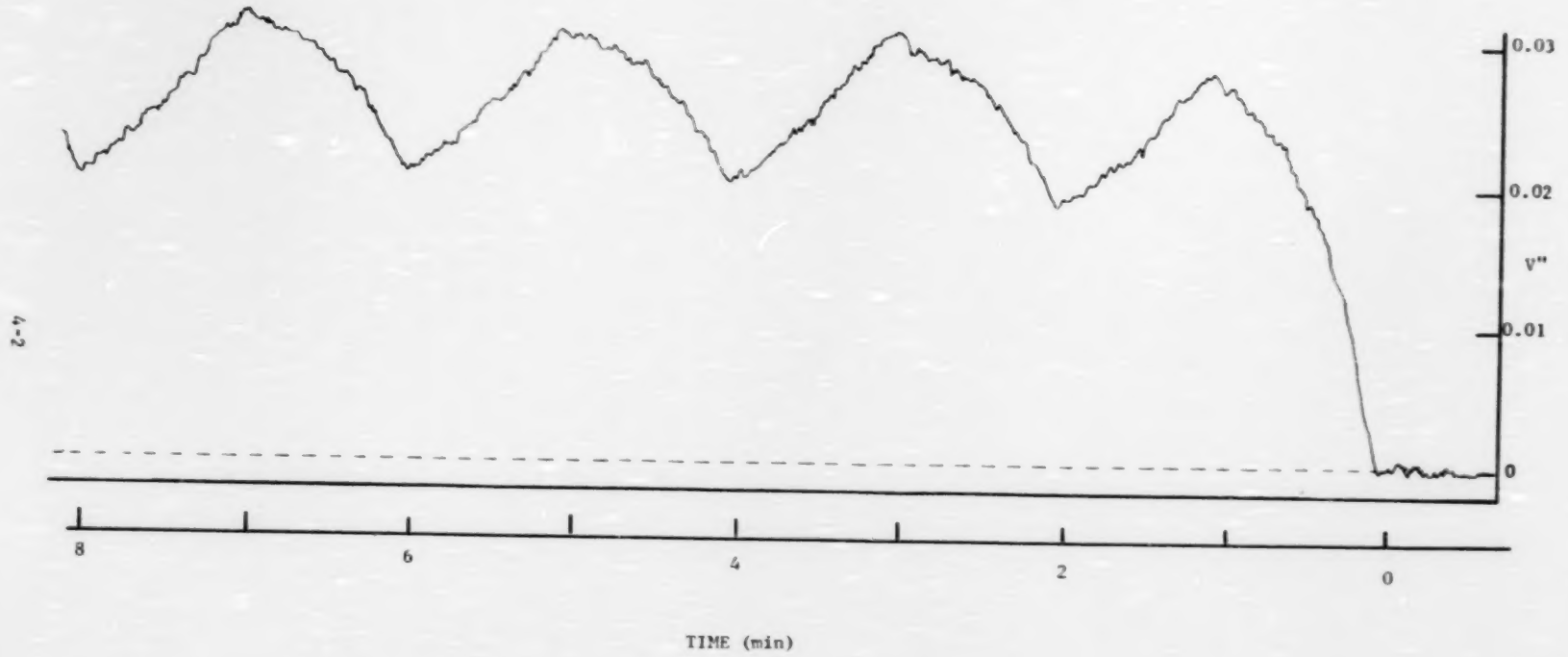

FIG. 4-1. Response of actinometer to solar energy with the shutter in the automatic mode.

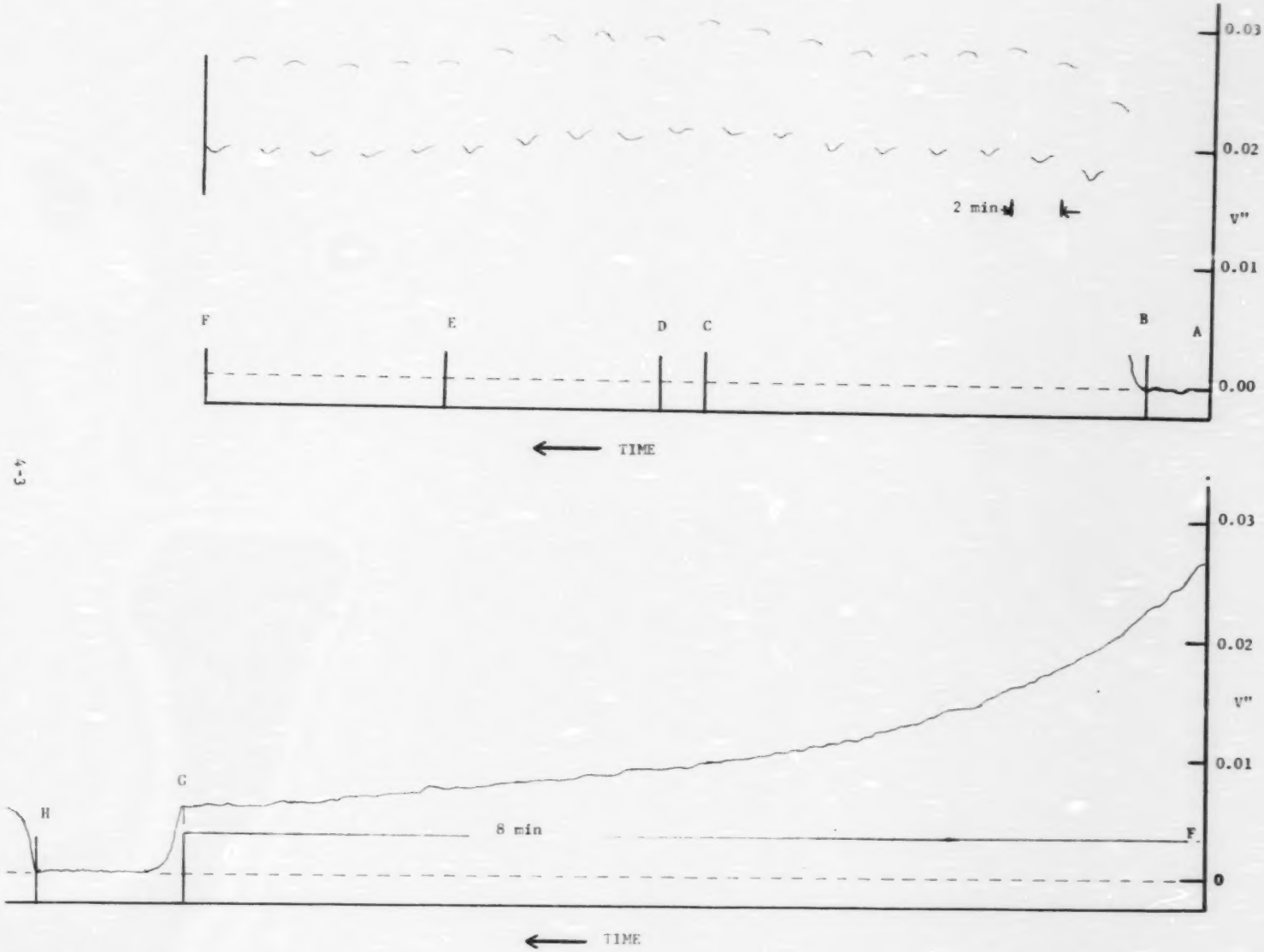

Fig. 4-2. Recorder tracings of actinometer output when the sky contains broken clouds. Upper panel: The shutter is cycling and the recorder chart drive and pen are in the automatic mode. Lower panel. The shutter is closed and the recorder is running continuously.

automatic mode. From point A to point B, the shutter has been closed sufficiently long that NO exists in the test bulb. At point B, both the recorder and shutter are started in the automatic mode. In this mode, the chart drives and the pen is in the writing position only for short periods when V" is near its minimum and maximum values. The shutter opens or closes during these short periods. Values of $\Delta V"$ can be determined from these condensed strips of chart by measuring between the minimum and maximum values of V" as illustrated in Fig. 2-2.

From point B to point C, the sky contained several broken clouds with some thin clouds moving into and out of the direct path between the sun and the test bulb. At point C, no apparent clouds were in the direct path. From point D to point E, a cloud formed in the path so that at point E there was enough scattering by the clouds that no apparent shadows were cast by trees or buildings in the neighborhood of the instrument. This type of cloud cover remained from point E to point F.

At point F, the shutter was closed and remained closed while the chart drove continuously and recorded the curve shown in the lower panel of Fig. 4-2. From point F to point G, V" decreased continuously, indicating a decrease in the concentration of NO in the test bulb. It is apparent that the rate of disappearance of NO decreases as its concentration decreases. Between points G and H the infrared monitoring beam was blocked in order to record the pen deflection corresponding to the absence of NO in the test bulb.

RESPONSE VS ACTINIC IRRADIANCE

The curve in Fig. 4-3 relates $\Delta V"$ to the relative actinic irradiance. A "black-light" placed approximately 20 cm from the test bulb served as the source of actinic energy to obtain the data on which the curve is based. A large, segmented chopper blade rotating at 1 revolution per second blocked the beam of actinic energy from the test bulb for different fractions of the time. The data point corresponding to a relative irradiance of 100 was obtained with this chopper blade stopped in the open position so that the test bulb was fully irradiated. By rotating the chopper with the blades adjusted so that the chopper was half open and half closed, it was possible to obtain the data point corresponding to a relative irradiance of 50. Similarly, a blade that blocked the beam 25% of the time was used for a relative irradiance of 75%, etc. Because of the 1 rps rate of the chopper blade the length of time that the beam was transmitted, or blocked, is short compared to the reaction time for the formation or decay or NO in the test bulb. Therefore, it is expected that decreasing the duty cycle in this manner has the same effect as decreasing the actinic irradiance by the same factor.

The non-linearity in the relationship between actinic irradiance and $\Delta V"$ arises from a combination of two factors. When the NO concentration

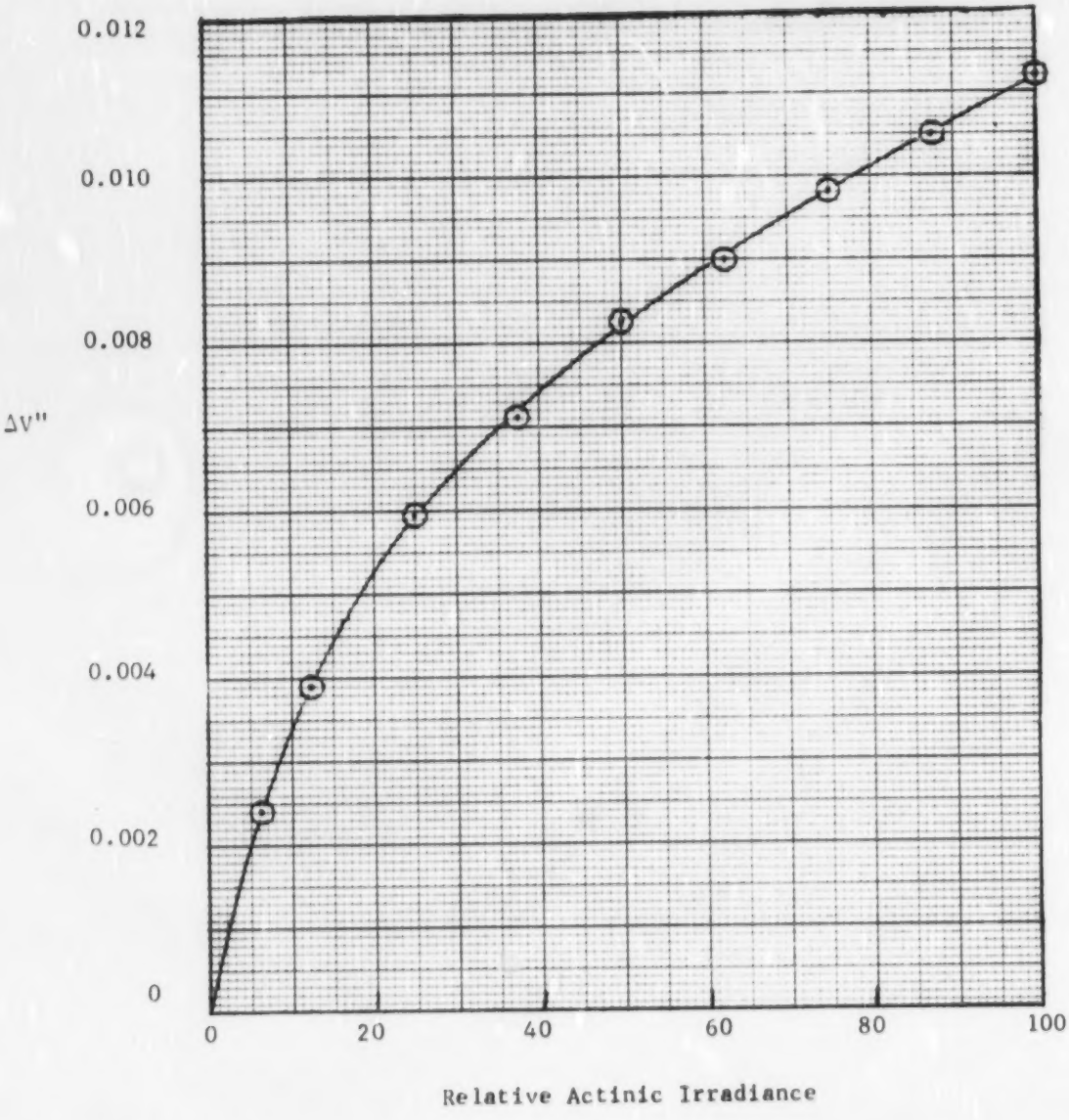

FIG. 4-3. Plot of ΔV" vs relative actinic irradiance.

in the test bulb is sufficiently high that the absorption is appreciable at the centers of the absorption lines, the amount of energy absorbed no longer increases linearly with the NO concentration. Secondly, the net rate at which NO is formed during each 1-minute period that the shutter is open decreases as the NO concentration increases. By reducing the period of the cycling shutter, the non-linearity resulting from the change in the rate of NO formation could be reduced. However, this would also reduce $\Delta V''$, and thus the signal-to-noise ratio.

RESPONSE VS DIRECTION OF ACTINIC ENERGY

As discussed in the first part of this section, we expect the response of the actinometer to be somewhat dependent upon its orientation relative to the sun, particularly when there are but a few clouds in the sky and most of the actinic energy arrives from a direction near the sun. In order to approximate the effect of direction we obtained the data summarized in Table 4-1 in the P.M. of May 1, 1974 when the sun was approximately 45^{o} above the horizon. The first measurement was obtained with the actinometer sitting on a horizontal table so that angle $\alpha = 0$. The long side of the actinometer was in the azimuthal direction of the sun with the end containing the test bulb farthest from the sun. The other data were obtained by rotating the actinometer clockwise around a vertical axis so that α was equal to the angles indicated. Approximately 10 minutes were required for the measurement at each angle. Three of four cycles of the shutter were used, and the data for all of the cycles were averaged.

As expected, the maximum response was observed when $\alpha = 0^{o}$, and the minimum occurred at $\alpha = 180^{o}$ when M9 provided the maximum shade on the test bulb. A few wispy clouds in the sky probably caused a few percent variation in the measurements. During the 50-60 minutes between the two times that the measurements were made at $\alpha = 0$, the change in $\Delta V''$ corresponded to approximately an 8% decrease in irradiance. Part of this decrease probably resulted from the increase in the zenith angle of the sun and the corresponding increase in the atmospheric path. Some of the decrease may have resulted from increased thickness of the thin clouds. Although the actinometer response is somewhat directional, a relatively small fraction of the energy is usually incident from the portion of the sky opposite the sun. Therefore, it is expected that errors due to the direction-dependent response will not exceed a few percent if the instrument is oriented as prescribed above with $\alpha = 0^{o}$.

TABLE 4-1

RESPONSE VS ORIENTATION OF ACTINOMETER RELATIVE TO THE SUN

Angle α (degrees)	ΔV"
0	0.0111
45	0.0109
90	0.0104
135	0.0099
180	0.0098
0	

RESPONSE VS NO CONCENTRATION

Although the quantity of primary interest is ΔV", it is also of interest to know the approximate concentration of NO in the test bulb at any time. Figure 4-4 shows a curve with which the NO concentration can be related to the instantaneous velue of V". The data on which the curve is based were obtained with mixtures of NO + N_2 in a sample cell in place of the test bulb. The absorber thickness of NO is equal to the partial pressure of NO in atmospheres times the optical path length of the sample cell. Since the optical path of the test bulb is approximately 21 cm, the NO concentration is (1/21) times the value of absorber thickness determined from Fig. 4-4 and the observed value of V". As an example, if V" = 0.02, the absorber thickness of NO is approximately 0.014 atm cm. This corresponds to a partial pressure of $0.014/21 = 0.67 \times 10^{-3}$ atm, or 0.9 torr of NO.

Because the absorption by a given absorber thickness of NO depends on the widths of the absorption lines, it depends on the collision frequency of the absorbing molecules and thus upon the total pressure of a mixture of NO with other gases such as NO_2, N_2, or O_2 that do not absorb in the spectral region where the NO is measured. The NO + N_2 mixtures used to obtain the data in Fig. 4-4 were adjusted to a total pressure of 120 torr, the same as that in the test bulb. Differences in the broadening abilities of N_2 and O_2 + NO_2 are not accounted for; however, they are expected to produce only slight errors when using Fig. 4-4 in the described manner to determine the concentration of NO in the test bulb.

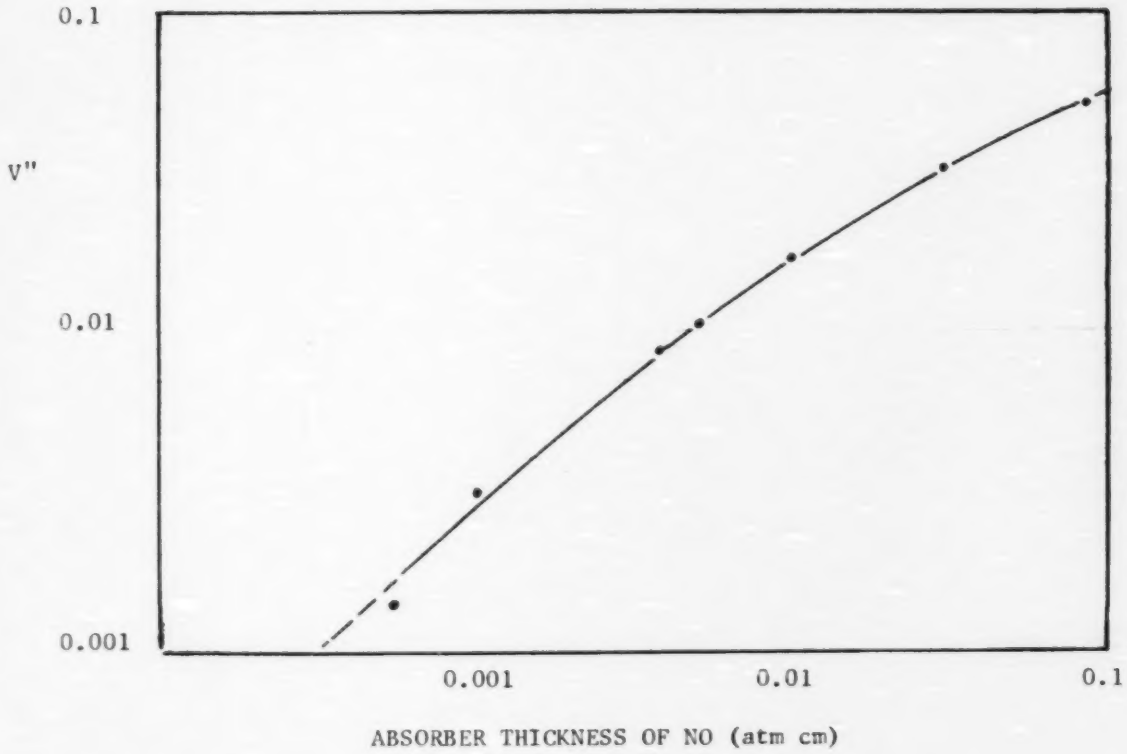

FIG. 4-4. Response of actinometer to different absorber thicknesses of NO in a mixture of NO + N_2 at a total pressure of 120 torr. By comparing the value of V" observed with the actinometer in normal use to this curve, it is possible to determine the NO concentration in the test bulb.

SECTION 5

ELECTRICAL DIAGRAMS AND DETAILS OF COMPONENTS

ELECTRICAL AND MECHANICAL

Figures 5-1 through 5-8 show schematic diagrams of the electrical components. These figures should be adequate for any trouble shooting, modifying or replacing of parts. The phase-lock amplifier has not been modified and is used in its normal manner. An input plug with a 1 K ohm resistor connected across the input leads has been added to the recorder.

Suppliers of the electrical and mechanical components and their specifications are listed below. Manufacturers' manuals are provided separately for the recorder and amplifier.

Recorder:	Hewlett-Packard Model 7123A with remote controls for the pen-lift and chart drive. Chart speeds 3.75 and 15 cm/min.
Amplifier:	Princeton Applied Research Model 122.
Power Supply:	Zeltec Model Z15AT100 DP. For the preamp and reference circuits.
Power Supply:	Powertec Model 2B5-3. For thermo-electric cooler for the detector.
Source Transformer:	Triad F-3X, 2.5 V ac @ 10 amp.
Timer Assembly:	Minarik Electric Company, multi-cam timer 6C-120S, recyling.

Chopper Motor:	Globe Industries, 75A-121-1.
Shutter Drive Motor:	Hurst Model GA, 5 rpm, synchronous, stock #171-01-043.
Clutch:	On shutter drive. PIC #R3-3-50.

OPTICAL COMPONENTS

Listed below are the specifications and the suppliers of the optical components:

Source:	Perkin-Elmer Part No. 457-0244. Operated in this instrument at approximately 2.5 V ac and 10 amps.
Detector:	InSb with 2 mm x 2 mm sensitive element cooled to approximately -25°C by a thermoelectric cooler. Optoelectronics Part No. OTC-3M1.
Test Bulb:	Quartz body with 1" diam CaF_2 windows. Windows and the line to the valve are bonded to the bulb with RTV, a silicone cement. Additional strength to the bonds is provided by epoxy cement. Because of a chemical interaction between epoxy cement and NO_2, the silicone is used to separate the epoxy from the NO_2 in the test bulb. A Monel valve connected to the test bulb makes it possible to refill the test bulb. The quartz body was provided by Quartz General, 12440 Exline Street, El Monte, Ca., 91732, who originally made it as a round bottom 500 ml flask. Cat. #W 106 Q.
Lens:	CaF_2, 1.37 cm diam, 1.39 cm effective focal length at 5.3 μm. Unique Optical, P.O. Box 585, Farmingdale, New York.
Mirrors M1 and M3:	5.0 cm diam, 10 cm focal length, spherical. Ealing Corporation, 2225 Massachusetts Ave., Cambridge, Mass., 021400.

M6:	5.0 cm diam, 10 cm focal length, spherical. Ealing Corporation.
Mirror M7:	Cut from a spherical mirror of 7.5 cm focal length provided by Ealing Corporation.
Mirror M9:	Cut to approximately 2.6 cm diam from a 7.5 cm focal length mirror provided by Ealing Corporation.
Mirrors M2, M4, M5, M8:	Flat mirrors cut to the desired dimensions.
Mirror Chopper:	Machined from stainless steel, chemically coated with aluminum and polished to provide a smooth finish. Contains 6 blades and revolves at approximately 3500 rpm producing a chopping frequency of 350 Hz.
Fixed Attenuator:	Sapphire window, 2.54 cm diam by 1 mm thick.

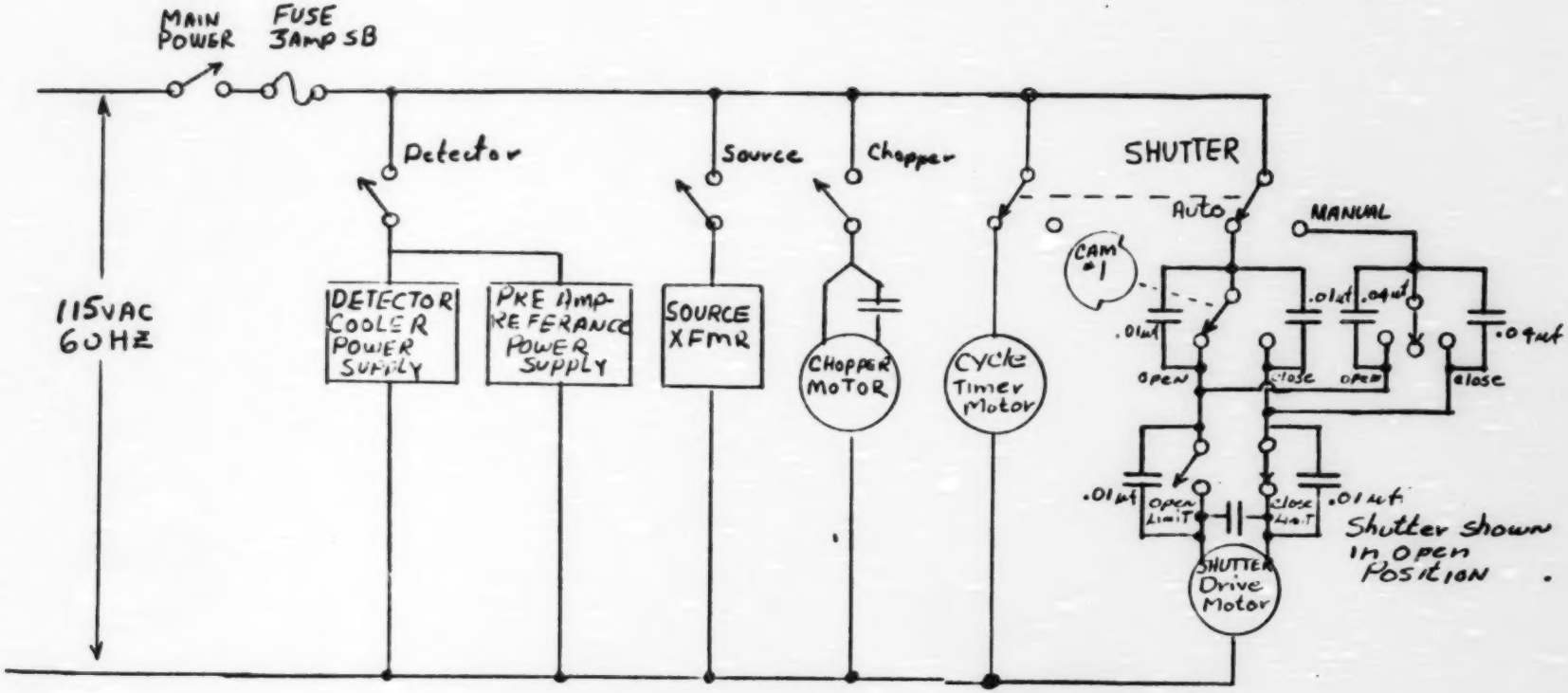

Fig. 5-1. Simplified schematic diagram for ac power. The shutter drive motor and its limit switches are located on the optics assembly; all other switches shown are on the control assembly. The power supplies, the transformer for the source and the chopper are on the optics assembly. The cycle-timer motor and the cams driven by it are in the control assembly.

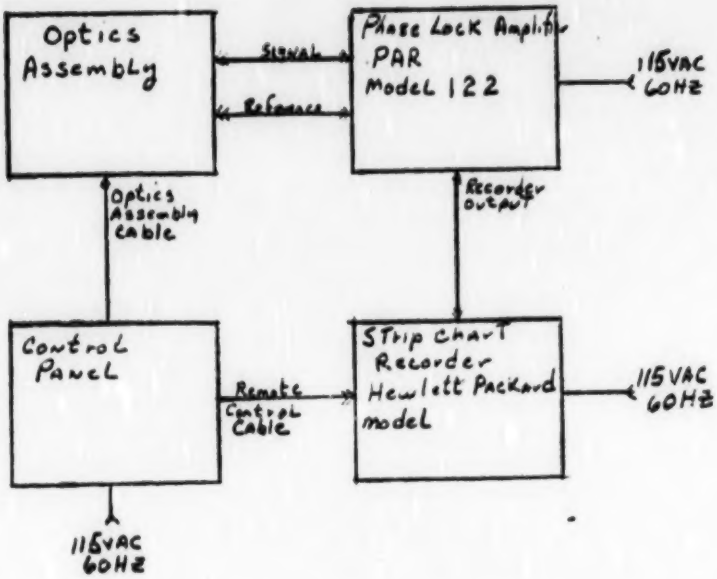

Fig. 5-2. Simplified diagram of interconnecting cables. It is recommended that the three separate lines for 115 V ac power be plugged into a common line. Cables connecting to the optics assembly are approximately 8 m long. The amplifier-recorder cable contains an 8-pin plug and is 1½ m long.

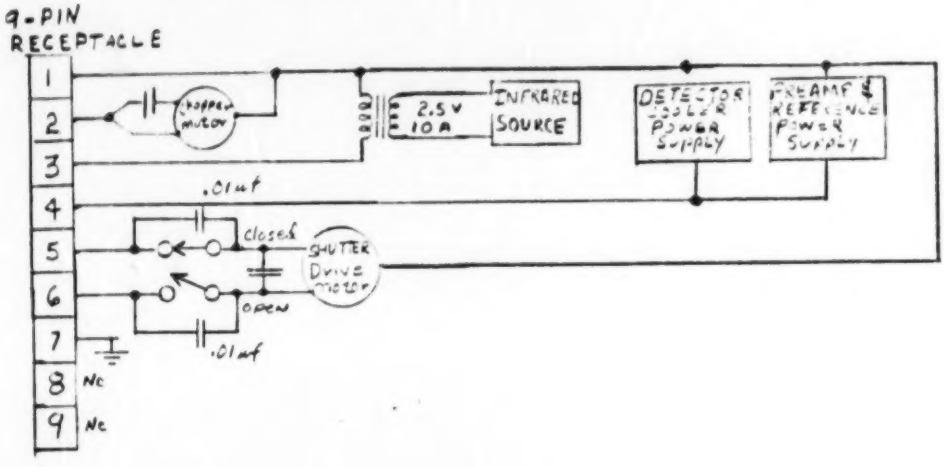

Fig. 5-3. Wiring diagram of electrical components on the optics assembly. The 115 V ac inputs for the power suppliers are shown; the output lines, not shown, go to the corresponding components.

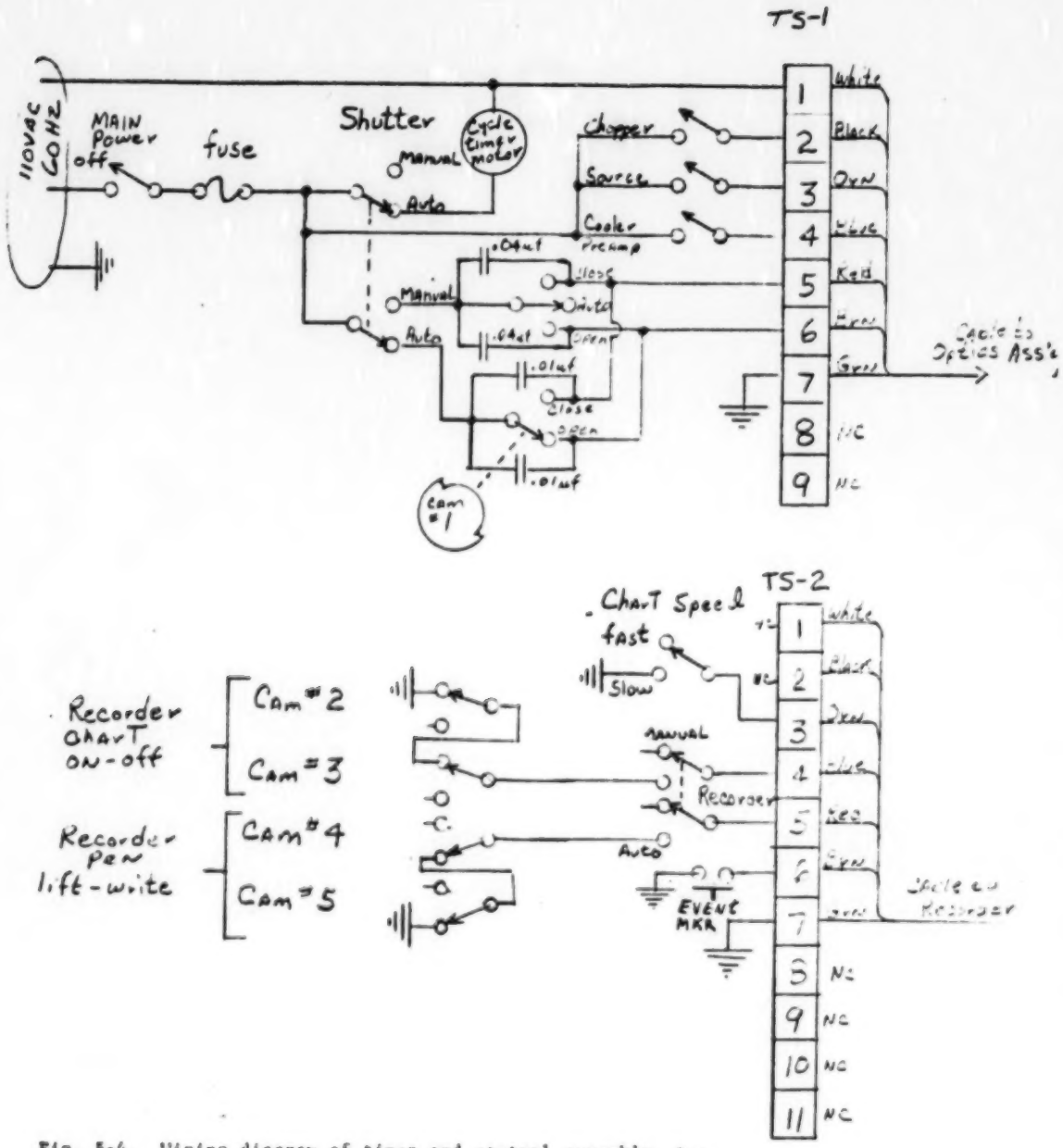

Fig. 5-4. Wiring diagram of timer and control assembly. One revolution of the cycle timer motor corresponds to one period of the shutter. Two interchangeable motors are provided; one runs at 1 rpm and the other at 0.5 rpm giving shutter cycles of 1 and 2 minutes, respectively. Cams 2 and 3 can be adjusted to change the period of time that the recorder chart switch is in the automatic position. Similarly, cams 4 and 5 control the pen lift. When the corresponding switches on the control assembly are in the manual position, the recorder chart drive and the pen lift are controlled by the switches on the recorder.

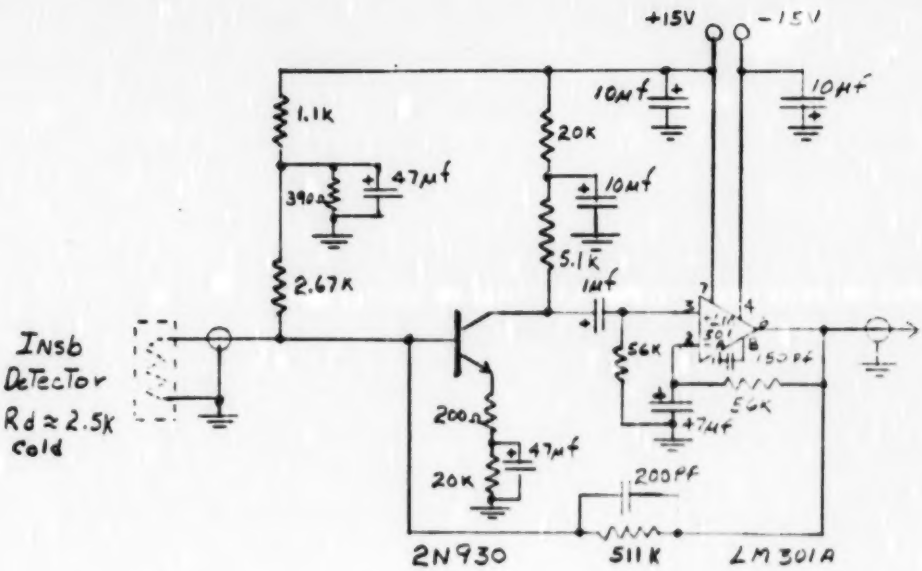

Fig. 5-5. Schematic diagram of preamplifier used with the InSb detector.

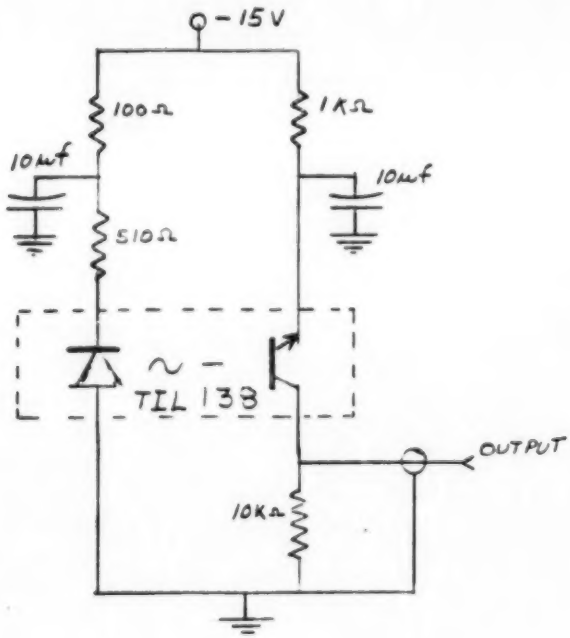

Fig. 5-6. Schematic diagram of the 350 Hz reference-pickup.

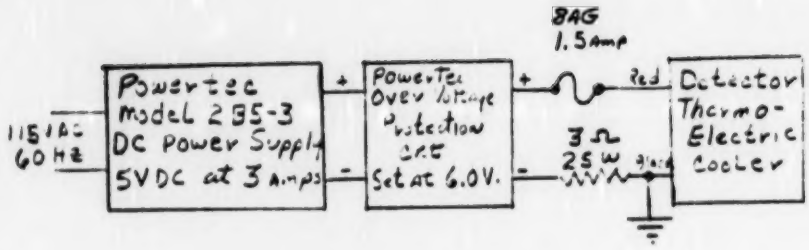

Fig. 5-7. Power supply for thermo-electric cooler for the detector.

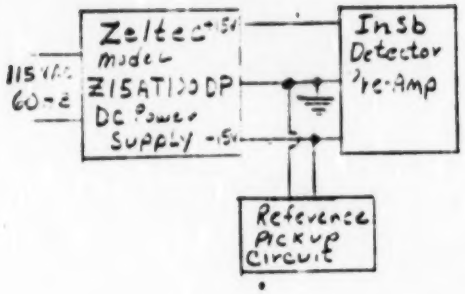

Fig. 5-8. Power supply for preamp and reference circuits.

SECTION 6

REFERENCES

1. Hanst, P. L., Environmental Protection Agency (private communication).

2. Leighton, Philip A., Photochemistry of Air Pollution, Academic Press, New York (1961).

3. Giauque, W. F. and Kemp, J.D. "The Entropies of Nitrogen Tetroxide and Nitrogen Dioxide. The Heat Capacity from 15 °K to the Boiling Point. The Heat of Vaporization and Vapor Pressure. The Equilibria $N_2O_4 = 2NO_2 = 2NO + O_2$." J. Chem. Phys. 6, 40 (1938).

4. Burch, D. E. and Pembrook, J. D. "Instrument to Monitor CH_4, CO, and CO_2 in Auto Exhaust." Report No. EPA-650/2-73-030. Prepared by Philco-Ford Corp., Aeronutronic Division for the Environmental Protection Agency. October 1973.

5. Hanst, P. L. "Spectroscopic Methods for Air Pollution Measurements," in Advances in Environmental Science and Technology. (New York: John Wiley and Sons, 1971).

6. Guttman, A. "Absolute Infrared Intensity Measurements on Nitrogen Dioxide and Dinitrogen Tetroxide." J. Quant. Spectrosc. Radiat. Transfer 2, 1 (1962).